

VOLUME 184 NUMBER 1 JANUARY 2023

INTERNATIONAL JOURNAL OF PLANT SCIENCES



THE UNIVERSITY OF CHICAGO PRESS

Special January 2023 Student Research Cover for the *International Journal of Plant Sciences*

Feature Article: Seago, James L., Jr, Kamal I. Mohamed, Breanna Leasure, and Nikole K. Bonacorsi. 2023. Engimatic Features of the Lycopodiaceae and Selaginellaceae – Lycopodophyta. *International Journal of Plant Sciences* 184: 34-55.

On the Cover: SUNY Oswego student Breanna Leasure co-authored this research article during her undergraduate years where, in December 2022-January 2023, she is still a student. She is shown at the Zeiss LSM700 laser confocal microscope at SUNY Oswego with a laser confocal image of a lycopod (*Phlegmariurus squarrosus*) stem that she prepared and photographed.

The background is Gray Woods along Gray Road in the Town of Minetto, New York, USA, where we were given permission to gather plants by Doren Norfleet. *Dendrolycopodium obscurum*, club moss or ground pine, is the plant growing through the leaf litter of the woods. There are four microscopic images of *Dendrolycopodium obscurum* from the article shown on the cover; these are three UV epifluorescent images and one 488 nm laser confocal image taken by Breanna Leasure, Kamal Mohamed, and James Seago.

We acknowledge the assistance of James Ellis, Christina Caruso, and Denise Howes, the University of Chicago Press, the *IJPS* journal, and SUNY Oswego in the development and construction of this special cover.



Left to right: Nikole, Kamal, Jim, Breanna

ENIGMATIC FEATURES OF THE LYCOPODIACEAE AND SELAGINELLACEAE—LYCOPODOPHYTA

James L. Seago Jr.,^{1,*†} Kamal I. Mohamed,[†] Breanna Leasure,[†] and Nikole K. Bonacorsi[‡]

*Seago Botanical Consulting, Minetto, New York 13115, USA; †Department of Biological Sciences, State University of New York, Oswego, New York 13126, USA; and ‡Manlius Pebble Hill School, Syracuse, New York 13214, USA

Editor: Julie Kang

Premise of research. We examined select members of the Lycopodiaceae (Lycopodioideae and Huperzioideae) and Selaginellaceae to determine whether there were some unique anatomical and histochemical traits that might contribute to our understanding of their stems and roots.

Methodology. Living plants and herbarium/dried specimens were examined using hand or hand microtome sections, processed in different stains, and viewed using different microscopic methods.

Pivotal results. Among the Lycopodiaceae, Lycopodioideae, the innermost region of the cortex in stems and roots often has variously modified cell walls that we term an endERMoid without Casparian bands. In the Huperzioideae, the cell walls of the innermost cortex usually have a layer of cells better defined as an endodermis because cells with Casparian bands are usually evident in a ring around the stele of stems and vascular cylinder of roots. Lycopodioideae adventitious roots have an epidermal emergence from the stems, while Huperzioideae roots have a cortical emergence. Stems of Selaginellaceae do not have a well-defined endodermis or endERMoid around their steles; instead, most species studied have an extracellular wall layer lining outer stele and inner cortical trabecular cells, interpreted as a stele-cortex wall that is readily apparent only under 488-nm laser microscopy. While most *Selaginella* species have an endodermis in their rhizophores, roots of all species studied have an endodermis with Casparian bands and often with suberin lamellae.

Conclusions. Our results revealed the occurrence of distinct innermost cortex layers not adequately and previously demonstrated in these plants. In Lycopodiaceae, these are endERMoid or endodermis. In Selaginellaceae, these are extracellular stele-cortex walls in most stems and endodermis in rhizophores and roots. There is clearly a need to examine in much greater detail cell wall chemistry and cell/tissue development as they relate to the genetics and molecular development of these extant lycopods and their phylogenetic history.

Keywords: lycopods, anatomy, unique features.

Introduction

Many years ago, this investigation began simply out of curiosity after J. L. Seago Jr. anatomically examined specimens of *Dendrolycopodium obscurum* and *Huperzia lucidula* living on the forest floor in mature woods along Gray Road in the town of Minetto, Oswego County, New York. We expanded the study to include a sampling of genera and species within the phylogenetic framework of the Lycopodophyta, basal Lycopodiaceae (Lycopodioideae and Huperzioideae), and Selaginellaceae (Wikström 2001; Zhou and Zhang 2015; Field et al. 2016; see also Lehnert et al. 2016; Westrand and Korall 2016; Zhou et al. 2016; Harrison

and Morris 2017; Mower et al. 2019; Spencer et al. 2021; Zhang et al. 2022).

The evolutionary history and anatomy of these terrestrial/epiphytic lycopods have long been studied (e.g., De Bary 1877, 1884; Sachs 1882; Van Tieghem and Douliot 1886; Strasburger et al. 1908; Gifford and Foster 1989; Thomas 1992; Kenrick and Crane 1997; Taylor et al. 2009; Banks et al. 2011; Christenhusz et al. 2011; Field et al. 2016; PPG 2016; Spencer et al. 2021; Stevens 2021). The evolutionary origin of roots in the plant body has been the subject of major reviews (e.g., Raven and Edwards 2001; Kenrick 2002), and the structure of the steles in the stems and roots has been well documented in extinct and extant vascular plants, lycopods, and euphyllophytes; studies of xylem cells have revealed some of the unique features of the cell wall structure and the differences between Lycopodiaceae and Selaginellaceae (e.g., Wilder 1970; Friedman and Cook 2000; Schneider and Carlquist 2000a, 2000b).

¹ Author for correspondence; email: jseago@twcny.rr.com.

Manuscript received April 2022; revised manuscript received September 2022; electronically published November 22, 2022.

The earliest somewhat definitive accounts of lycopod anatomy related to ground tissues were by Hegelmaier (1872), Bower (1885, 1894), De Bary (1877, 1884, p. 349, fig. 162, with an unlabeled ring in the position of the endodermis), and Harvey-Gibson (1894, 1896, 1897, 1902; Mitchell 1910). The innermost layer of the cortex was termed the phloeoterma and starch sheath by Strasburger et al. (1908), especially when starch grains dominated the cells of the layer and no Casparian bands were evident. Jones (1905, fig. 2; only a “diagrammatic drawing” with the endodermis labeled; not shown in photographs) and Sinnott (1909; no endodermis shown or labeled in the stem or its leaf traces) were among the first to illustrate the anatomies of the lycopods with photographs. Even after those articles, photographs of anatomical structures were often not presented in articles (e.g., Hill 1914; Barclay 1931). Nevertheless, the anatomy of lycopod stems, leaves, and roots has been thoroughly summarized in classical references by Ogura (1972; see also Jones 1905; Hill 1914; Barclay 1931; Freeburg and Wetmore 1967; Gifford and Foster 1989; Fahn 1990; Gola et al. 2007; Beck 2010; Roy et al. 2013; Gola and Jernstedt 2016; Spencer et al. 2021). Lycopodiaceae steles can be considered monosteles or protosteles (haplosteleles, actinosteles, and plectosteles). However, some Selaginellaceae are monostelic, but most are polystelic, and each separate bundle or stele in a polystelic stem is a meristele (Ogura 1972; Fahn 1990; Gola and Jernstedt 2016). It was not our purpose to reinvestigate the general anatomy and vascular patterns of the lycopod Lycopodiaceae and Selaginellaceae because this has been done by many researchers over the past 150 years (above citations).

The presence of an endodermis in lycopods has long been in question. Major morphological and anatomical treatments in books like those by Gifford and Foster (1989) and Bierhorst (1971) did illustrate an endodermis with photographs, but without evident Casparian bands. Bierhorst (1971, p. 10, fig. 2-2A) labeled an endodermis in a *Lycopodium serratum* (synonym, *Huperzia serrata*) stem with a slightly thickened inner tangential wall of his END-labeled layer or outer tangential wall layer of a pericycle; he did not label a layer as endodermis in the lycopod roots. Ogura (1972, p. 43) noted that in *Lycopodium* and Isoetaceae, “a special layer corresponding to the endodermis is seen in a young stage, but during the growth its characteristic is lost, and in the adult stage it is no more recognizable.” He also had multiple illustrations of *Lycopodium* and *Selaginella* structures, but most were copies of Harvey-Gibson drawings (especially from Harvey-Gibson 1894). In their definitive tome on vascular plant morphology, Gifford and Foster (1989, p. 111) stated that “endodermis with casparian strips is not evident” in the Lycopodiales, whereas in stems of Selaginellales, “radially elongated endodermal cells designated *trabeculae* . . . have the characteristic casparian strips.”

Lycopodium has been reported to be the only genus of such vascular plants to lack an endodermis with Casparian bands in the roots (e.g., Damus et al. 1997; Enstone et al. 2003), although Bierhorst (1971, p. 10, fig. 2-2A) reported and photographed a labeled endodermis around the stele in *L. serratum* (now *H. serrata*) but not in its roots (Bierhorst 1971, pp. 10–11, fig. 2-2A, 2-3C, 2-3D). However, endodermis was present in *Selaginella* (roots: Damus et al. 1997; stems: McLean and Juniper 1979; Pita et al. 2006; Schulz et al. 2010; Gola and Jernstedt 2016). Scott (1904, p. 12, fig. 8) drew inner cortical trabeculae with a

Casparian band in one long cell and multiple trabecular cells, with the innermost cell having a Casparian band and being directly connected to a cell that extends beyond a so-called pericycle with a thick outer tangential wall (all redrawn, with slight but significant differences, from Harvey-Gibson 1894, fig. 46). Ogura (1972, p. 193) noted that “usually the cell wall of the pericycle round the lacuna is more or less cutinized” and that the endodermis occurs in various ways in the equally variable lacunar inner cortex of different *Selaginella* species. McLean and Juniper (1979, figs. 1–12) used electron microscopy to illustrate Casparian bands in *Selaginella kraussiana*, and they described the outer walls lining the pericycle and trabeculae as cuticle without demonstrating their chemical nature. The innermost layer or layers of the cortex have not been well documented, except by Harvey-Gibson (1894), and the illustrations in Barclay (1931, fig. 1) and McLean and Juniper (1979, figs. 1, 3) do not clearly demonstrate the origin of the cells and the associated files of cells from the meristem.

Herein, we report observations of the structure of the shoots (mostly stems) and roots as they relate to each other, the similarities or differences in their general structure, and, specifically, the inner cortex barrier layers in selected members broadly representing some major clades within the Lycopodiaceae and Selaginellaceae. Our main goal is to examine the relationship and structures of the innermost layer(s) of the cortex around the stem steles and root vascular cylinders, with limited developmental analyses, and to determine whether there is an endodermis (with distinct Casparian bands), an endodermoid (with modified cell walls but not distinct Casparian bands), or an extracellular stele-cortex wall bordering the stele and cortex using a variety of histochemical and microscopic methods. Our sampling should give researchers foundations for more in-depth analyses of these structures and their genetic/molecular foundations and chemical compositions.

Material and Methods

The family, subfamilies, genera, and species we studied (Wikström 2001; Zhou and Zhang 2015; Field et al. 2016) are as follows.

Lycopodiaceae. Lycopodioideae: *Lycopodium clavatum* L., *Lycopodiella inundata* (L.) Holub (synonym, *Lycopodium inundatum*), *Diphasiastrum complanatum* (Michaux) Trevisan (synonym, *Lycopodium complanatum*), and *Dendrolycopodium obscurum* (L.) Haines (synonym, *Lycopodium obscurum*).

Huperzioidae. *Huperzia lucidula* (G. Forst.) Á. Löve & D. Löve (synonym, *Lycopodium lucidulum*) and *Phlegmariurus squarrosus* (synonyms, *Lycopodium squarrosus*, *Huperzia squarrosa*).

Selaginellaceae. Subgenus *Boreoselaginella*: *Selaginella borealis* (Kaulf.) Spring (synonym, *Lycopodium boreale*). Subgenus *Ericetorum*: *Selaginella kraussiana* (Kunze) A. Braun (synonym, *Lycopodium kraussianum*) and *Selaginella lepidophylla* Hooker & Greville (synonym, *Lycopodium lepidophyllum*). Subgenus *Heterostachys*: *Selaginella uncinata* (Desvaix ex Poir.) Spring (synonym, *Lycopodium uncinatum*). Subgenus *Stachygyndrum*: *Selaginella moellendorffii* Hieron.

Most specimens were harvested directly from plants grown in the wild or obtained commercially and grown in pots kept in the State University of New York at Oswego greenhouse. Because we had access to forests in the towns of Minetto, Granby, and Parish

(Oswego County, NY) with so many of *D. obscurum*, *D. complanatum*, and *H. lucidula* plants, we were able to harvest, section, stain, and examine many individuals to provide more details of their structure. Material of *L. clavatum* and *L. inundata* was taken from herbarium sheet specimens, cut into 5–10-mm-long pieces, placed in 10% glycerine in H₂O for at least 24 h, and then rinsed in dH₂O prior to sectioning and staining; we also contrasted this with just soaking dried specimens in tap water and determined that these specimens could be used too. Stems and roots were sectioned freehand with razor blades under a Zeiss dissecting microscope or in hand microtomes with stem or root pieces positioned between moistened pieces of *Sambucus* pith and cut with a hand microtome blade. Sections were then stained—for example, with berberine hemisulfate—for at least 1 h, rinsed, and viewed or counterstained in aniline blue, gentian violet, or toluidine blue O. Or they were stained in fluorol yellow, Sudan red 7B, or Sudan IV for 1 h and phloroglucinol-HCl for 5 min and digested in acid with 65% H₂SO₄ (but no acid digestion or Sudan red 7B images are shown here). These procedures and treatments were done according to Brundrett et al. (1988, 1991), Seago et al. (1999), Lux et al. (2005), Zelko et al. (2012), Soukup (2014), or Seago (2020). The sections on microslides were variously viewed using a Zeiss LSM700 bright-field microscope, UV epifluorescence, a 488-nm laser confocal microscope, or differential interference contrast microscopy.

Terminology. Terminology for the stele, cortex, and endodermis has been an issue for many years, since the studies by Caspary (1858), Van Tieghem and Douliot (1886), and De Bary (1884). For example, Caspary originally termed it a *Schüttscheide*, but De Bary (1884) started the general use of the term “endodermis” for cells in a layer of the innermost cortex that have lignified Casparian bands in transverse and radial cell walls (von Guttenberg 1943; Enstone et al. 2003; Soukup and Tylová 2018). While the term “Casparian strip” is often used, we use “Casparian band” in accordance with Schreiber (1996), Schreiber et al. (1999), Enstone et al. (2003), Schreiber and Franke (2011), Soukup and Tylová (2018), and Seago (2020).

An endodermis with Casparian bands made mostly or entirely of lignins is an apoplastic barrier in radial and transverse primary cell walls (Towers and Maass 1965; Schreiber et al. 1999; Enstone et al. 2003; Espiñeira et al. 2011; Schreiber and Franke 2011; Naseer et al. 2012; Soukup and Tylová 2018). Esau (1977, p. 259) used the term “endodermoid” as the adjective form of “endodermis”; however, for most authors, “endodermal” is the preferred adjective for endodermis (see, e.g., Gifford and Foster 1989; Enstone et al. 2003; Geldner 2013; Seago and Fernando 2013; Soukup and Tylová 2018, etc.). We use the term “endodermis” only where multiple procedures demonstrate Casparian bands or such wall-like modifications of cell walls in a layer (or layers; there is sometimes overlap of cells or layers because of section thickness or development) via a combination of stains and microscopy, even without apoplastic permeability tests, which we could not perform. In typical plants like angiosperms, these Casparian bands are composed primarily of lignins, with small amounts of suberin (Schreiber and Franke 2011).

An endodermoid is a circumferential cylinder, layer, or ring of cells of the innermost cortex (often a few cells wide) around the stele with various cell wall modifications (see “Results” and “Discussion”); conspicuous Casparian bands are not easily demonstrable in an endodermoid. We will use the noun “endodermoid”

when our multiple staining and microscopy procedures do not, with certainty, result in the agreement that Casparian bands are present and demonstrable in the innermost layer(s) of cortex. We do not know the kinds of lignins or other compounds.

A stele-cortex wall is an extracellular layer outside the primary cell walls, present on the surfaces of the outer stele and inner cortex trabecular cells in an uneven or undulating layer. Chemically, it is probably cutin or suberin.

The endodermoid and stele-cortex wall are not endodermis with manifest Casparian bands (Soukup and Tylová 2018; Seago 2020). Terms like “starch sheath” and “bundle sheath” for an inner layer of cortex or mesophyll have also been included under endodermis (see discussion by Geldner 2013, pp. 532–533, 553), but they are not applicable here.

Results

The various species of the Lycopodiaceae, Lycopodioideae, and Huperzioidae are presented in figures 1–5 and the species of Selaginellaceae in figures 6–8 (see table 1 for a list of the abbreviations used in the figures). In the specimens we sectioned, we observed stems with adventitious root and leaf traces, adventitious roots, rhizophores and dichotomized roots, and a few microphylls.

Lycopodiaceae, Lycopodioideae. *Lycopodiella inundata* herbarium specimens (fig. 1A–1F) were variable; a stem actinoplectostele stained in berberine or counterstained in gentian violet or aniline blue under UV epifluorescence (fig. 1A) was ringed by an endodermoid of the innermost cortex, with sclerenchymatous cells particularly evident in the middle cortex in berberine aniline blue (fig. 1A) and gentian violet sections. That stem inner cortex endodermoid and the attached microphyll leaf trace endodermoid were clear in thin, variously positioned, fluorescing walls under higher magnification in berberine aniline blue epifluorescence (fig. 1B). Under laser confocal microscopy with berberine gentian violet staining (fig. 1C, 1D), an endodermoid was conspicuous because of its uneven, undulating, and overlapping cells, sometimes with no inner cortical sclerenchyma in some specimens (fig. 1C). In adventitious roots (fig. 1E, 1F), evident endodermoid surrounded the vascular cylinder. Under laser confocal microscopy (fig. 1E), the endodermoid in the proximal roots exhibited thinner cell walls than the midcortex sclerenchymatous cells and was clearly differentiated from outer vascular cylinder regions, whereas in distal sections under UV epifluorescence (fig. 1F), the endodermoid had rings of cells with more or less brightly fluorescing cells.

Adventitious roots of *Lycopodium clavatum* plants (fig. 1G–1M; herbarium and dried specimens) exhibited perpendicular growth from the stele with epidermal emergence (fig. 1G); the plectostele nature of the stem (fig. 1G, 1H, 1J) was evident. Under berberine (fig. 1G) and berberine aniline blue epifluorescence, there was no good evidence of endodermoid cell wall modifications in the innermost cortex, but the inner and outer stem cortex had sclerified cell walls. Under berberine gentian violet laser confocal microscopy (fig. 1H, 1I) and epifluorescence (fig. 1J, 1K), the ring of cells in the inner cortex exhibited cell wall modifications in laser (fig. 1H, 1I) and fluorescent (fig. 1J, 1K) images; the immediately adjacent inner cortex exhibited tangentially flattened and thicker (fig. 1J) cell walls. Proximal adventitious roots exhibited a zone of cells that represents an endodermoid at the

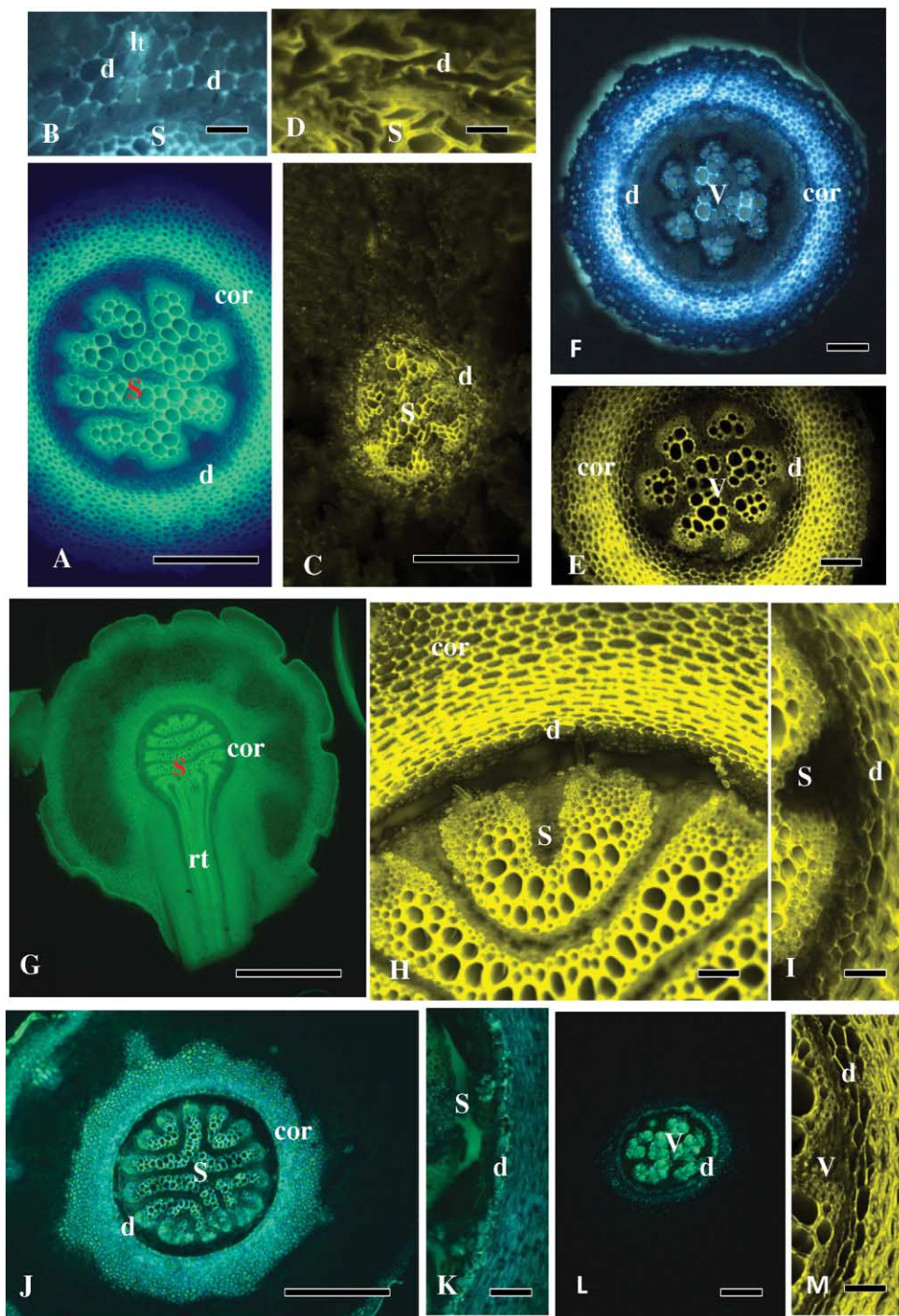


Fig. 1 A–F, *Lycopodiella inundata*. A, Stem and cortex with endodermoid around the stem actinostele, BABef. Scale bar = 130 μ m. B, Higher magnification of A, endodermoid outside the stele and around the leaf trace, BABef. Scale bar = 50 μ m. C, Stem and irregular endodermoid around the stem actinostele, BGVlc. Scale bar = 250 μ m. D, Close-up of the edge of a stem stele with irregular endodermoid cell walls, BGVlc. Scale bar = 40 μ m. E, Proximal root, cortex, actinostele, and endodermoid with thinner walls than in adjacent cortical cells, BGVlc. Scale bar = 100 μ m. F, Distal root and fluoresced endodermoid at the inner edge of the cortex, BGVef. Scale bar = 100 μ m. G–M, *Lycopodium clavatum*. G, Stem, plectosteles, and broad cortex. The inner cortex and outer cortex are sclerenchymatous, the adventitious root trace is perpendicular to the stele and emerged through the epidermis, and there is epidermal cuticle, Bef. Scale bar = 1300 μ m. H, Stem with plectosteles and thick-walled cortex layers and endodermoid, BGVlc. Scale bar = 130 μ m. I, Close-up of a stem endodermoid with thinner walls than the adjacent sclerenchyma of the cortex, BGVlc. Scale bar = 60 μ m. J, Stem with plectosteles and sclerenchymatous cortex, BGVef. Scale bar = 420 μ m. K, Close-up of the stem stele and endodermoid with variously modified and fluorescent cell walls, BGVef. Scale bar = 60 μ m. L, Adventitious root and actinostelic vascular cylinder with surrounding endodermoid, BGVef. Scale bar = 80 μ m. M, Adventitious root close-up with variously thickened endodermoid cell walls thinner than adjacent cortex cells to the right, BGVlc. Scale bar = 60 μ m. See table 1 for definitions of abbreviations.

Table 1

Glossary of Abbreviations

Abbreviation	Definition
Abbreviations on photos:	
c	Epidermal cuticle
cor	Cortex
d	Endodermoid
e	Endodermis
h	Root/rhizophore hairs
lt	Microphyll leaf trace
rt	Adventitious root trace
S	Stem stele
t	Trabecula
V	Root vascular cylinder
w	Stele/cortex wall
Abbreviations for stains and microscopies in legends:	
B	Berberine
BAB	Berberine aniline blue
BGV	Berberine gentian violet
BTBO	Berberine toluidine blue O
FY	Fluorol yellow
PG	Phloroglucinol
SIV	Sudan IV
TBO	Toluidine blue O
UNST	Unstained
bf	Bright field
dic	Differential interference contrast
ef	UV epifluorescence
lc	488-nm laser confocal

inner cortex outside the actinostelic vascular cylinder (fig. 1L); distal adventitious roots had a smaller actinostelic vascular cylinder with an endodermoid under berberine gentian violet epifluorescence. Endodermoid cells in stems and roots had no Casparian band. Unstained and berberine gentian violet laser confocal (fig. 1M) images revealed a thick-walled inner cortex outside the endodermoid, but this region of thick-walled cells was not evident in berberine gentian violet epifluorescence images (fig. 1L).

In *Diphasiastrum complanatum* (except for the microphylls; fig. 2A), we observed that under different treatments—berberine gentian violet epifluorescence (fig. 2B, 2C), berberine gentian violet laser confocal microscopy (fig. 2D), toluidine blue O (fig. 2E), unstained bright-field microscopy (fig. 2F), unstained epifluorescence (fig. 2G), and berberine or berberine toluidine blue O epifluorescence (both not shown)—green stems (fig. 2B–2E) and rhizomes (fig. 2F–2I) exhibited the same broad ring of inner cortex, or multilayered endodermoid, that presented different images under epifluorescence or laser confocal microscopy, with thin radial or thick tangential walls and more prominent cell corners where there were no intercellular spaces (fig. 2H, 2I). Typical for the lycopods, microphylls (fig. 2A) did not have such an endodermoid. There was no evidence of suberin under Sudan red 7B (not shown). Adventitious roots arose perpendicularly from the stele and had an epidermal emergence (fig. 2J), and they already had a visible endodermoid ring under berberine gentian violet epifluorescence (fig. 2J); in the proximal roots, this ring (fig. 2K) was somewhat similar to that of stems under laser confocal imaging (as in fig. 2I). In distal adventitious roots, berberine gentian violet epifluorescence specimens showed an endodermoid

(fig. 2L), and unstained laser confocal specimens revealed an irregular zone of tangentially thick-walled endodermoid cells (fig. 2M); sections stained and viewed in berberine gentian violet fluorescence had an endodermoid that exhibited walls that resembled Casparian bands (fig. 2N). The vascular cylinder of these roots exhibited a plectostele or an actinostele at proximal (fig. 2J, 2K) and distal (fig. 2L) root levels and exhibited thick-walled cortex under laser confocal microscopy (fig. 2K).

Dendrolycopodium obscurum strobilus axes (fig. 3A) and microphylls had no endodermoid. Within 5 mm of the vegetative stem tip, green stems had an endodermoid (fig. 3B) and little mature xylem; within 50 (fig. 3C) to 1000 mm (fig. 3D), the stele had two to four strands of xylem and had a distinct endodermoid in berberine gentian violet laser confocal (fig. 3C) and epifluorescence (fig. 3D, 3E) images. Then the stele became mostly plectostelic (fig. 3F); the endodermoid was quite distinct under berberine gentian violet epifluorescence (fig. 4F, 4G), even appearing to have Casparian band-like walls in some cells (fig. 3G), but without distinct endodermoid under berberine epifluorescence (fig. 3H) or unstained laser confocal microscopy (fig. 3I). Berberine epifluorescence specimens (fig. 3J) showed an endodermoid around stele and microphyll leaf traces. In the brown rhizomes of *D. obscurum*, under fluorol yellow epifluorescence (fig. 3K) and in unstained epifluorescence (not shown), an endodermoid was faint and not distinct, but in berberine epifluorescence (fig. 3L, 3M), it was distinct, with some Casparian-like bands (fig. 3M). The perpendicular origin of adventitious roots from the stem stele was via epidermal emergence (fig. 3N). When adventitious roots first emerged (fig. 3O), the vascular cylinder

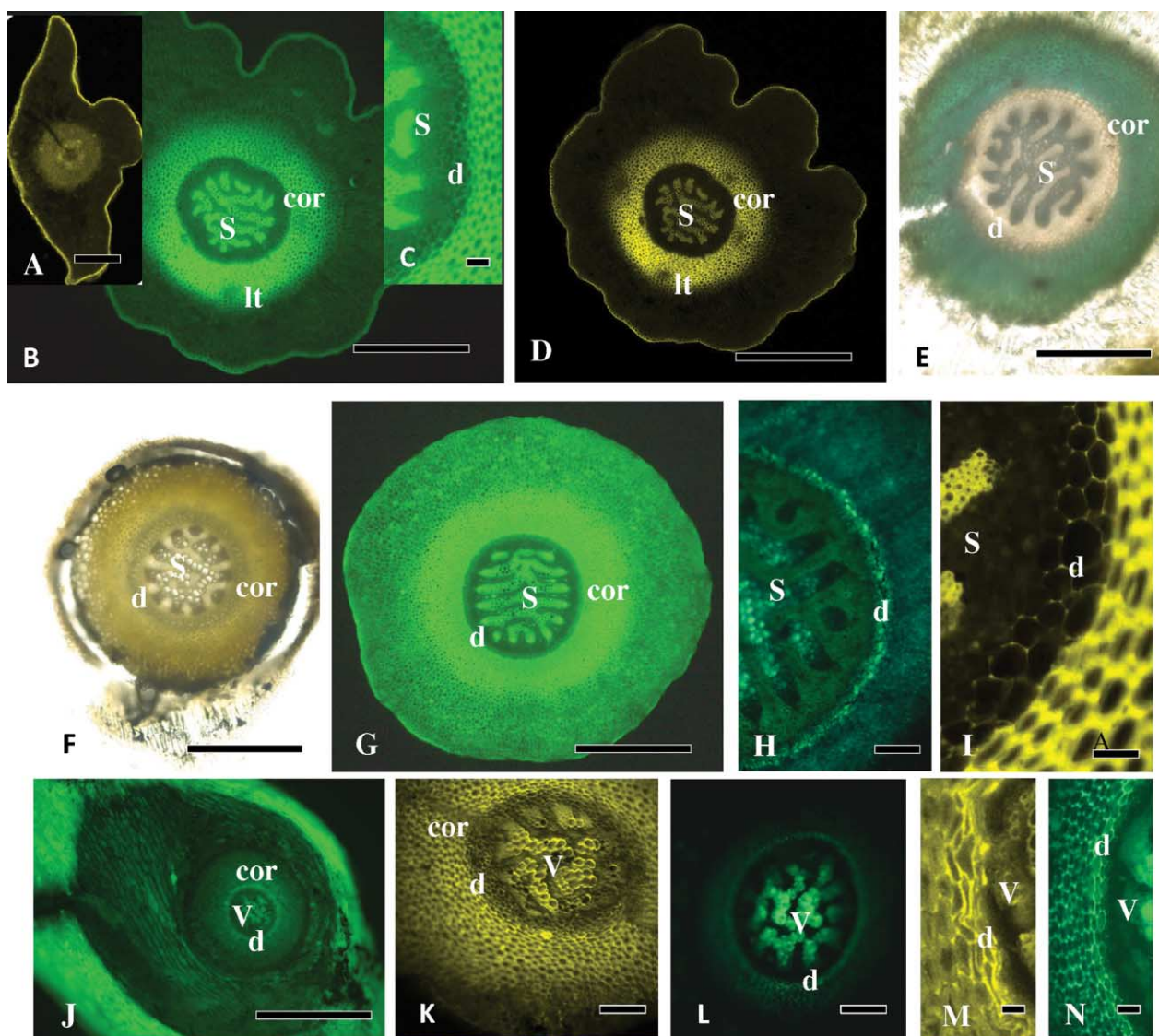


Fig. 2 *Diphasiastrum complanatum*. *A*, Microphyll section and no endodermoid, PGlc. Scale bar = 400 μm . *B*, Green stem, cortex, microphyll trace, and plectostele, BGVef. Scale bar = 1400 μm . *C*, Close-up of stem, edge of stele, and endodermoid, BGVef. Scale bar = 100 μm . *D*, Stem, BGVlc. Scale bar = 1200 μm . *E*, Green stem with cortex and innermost zone of endodermoid, TBObf. Scale bar = 500 μm . *F*, Rhizome, stele, and endodermoid, UNSTbf. Scale bar = 500 μm . *G*, Rhizome, plectostele, cortex, and faint endodermoid, UNSTef. Scale bar = 1200 μm . *H*, Rhizome, stele, and endodermoid, BGVef. Scale bar = 150 μm . *I*, Rhizome, edge of stele, endodermoid with thin cell walls, and some conspicuous radial walls, BGVlc. Scale bar = 60 μm . *J*, Adventitious root at its origin through the epidermis of the stem, vascular cylinder, cortex, and endodermoid, BGVef. Scale bar = 600 μm . *K*, Proximal adventitious root, cortex, vascular cylinder, and endodermoid, BGVlc. Scale bar = 150 μm . *L*, Distal adventitious root, vascular cylinder, and endodermoid, BGVef. Scale bar = 300 μm . *M*, Close-up of adventitious root, vascular cylinder, and variously thickened walls, especially tangential walls, of the endodermoid, UNSTlc. Scale bar = 30 μm . *N*, Close-up, adventitious root, vascular cylinder, and endodermoid, BGVef. Scale bar = 35 μm . See table 1 for definitions of abbreviations.

was very similar to the plectostele of stem steles; in long roots, diarchy (fig. 3*P*) or incomplete diarchy (fig. 3*Q*) was normal. The endodermoid was not very evident in unstained epifluorescence (fig. 3*P*; berberine, berberine aniline blue, and fluorol yellow epifluorescence not shown), but it was very distinct in berberine gentian violet, even appearing to have Casparian bands (fig. 3*Q*). The cortex in young stems had little cell wall thickening (fig. 3*B*–3*D*), but in older stems and roots, the cortex was usually thicker walled (fig. 3*H*, 3*I*, 3*N*), except that berberine epifluorescence-imaged

stems and roots (fig. 3*L*, 3*Q*) did not show such thick walls outside the endodermoid.

Huperzioidae: *Huperzia lucidula*. In a young terminal stem of *H. lucidula*, an incipient microphyll leaf trace, a leaf trace in the cortex, and the stem stele (fig. 4*A*) were enclosed by an irregular endodermoid zone in berberine epifluorescence; some cells may have had Casparian bands (leaf traces). The xylem did not extend across the stele (fig. 4*A*). The young stem mostly had four xylem bundles in an actinostelic configuration (fig. 4*B*; unstained

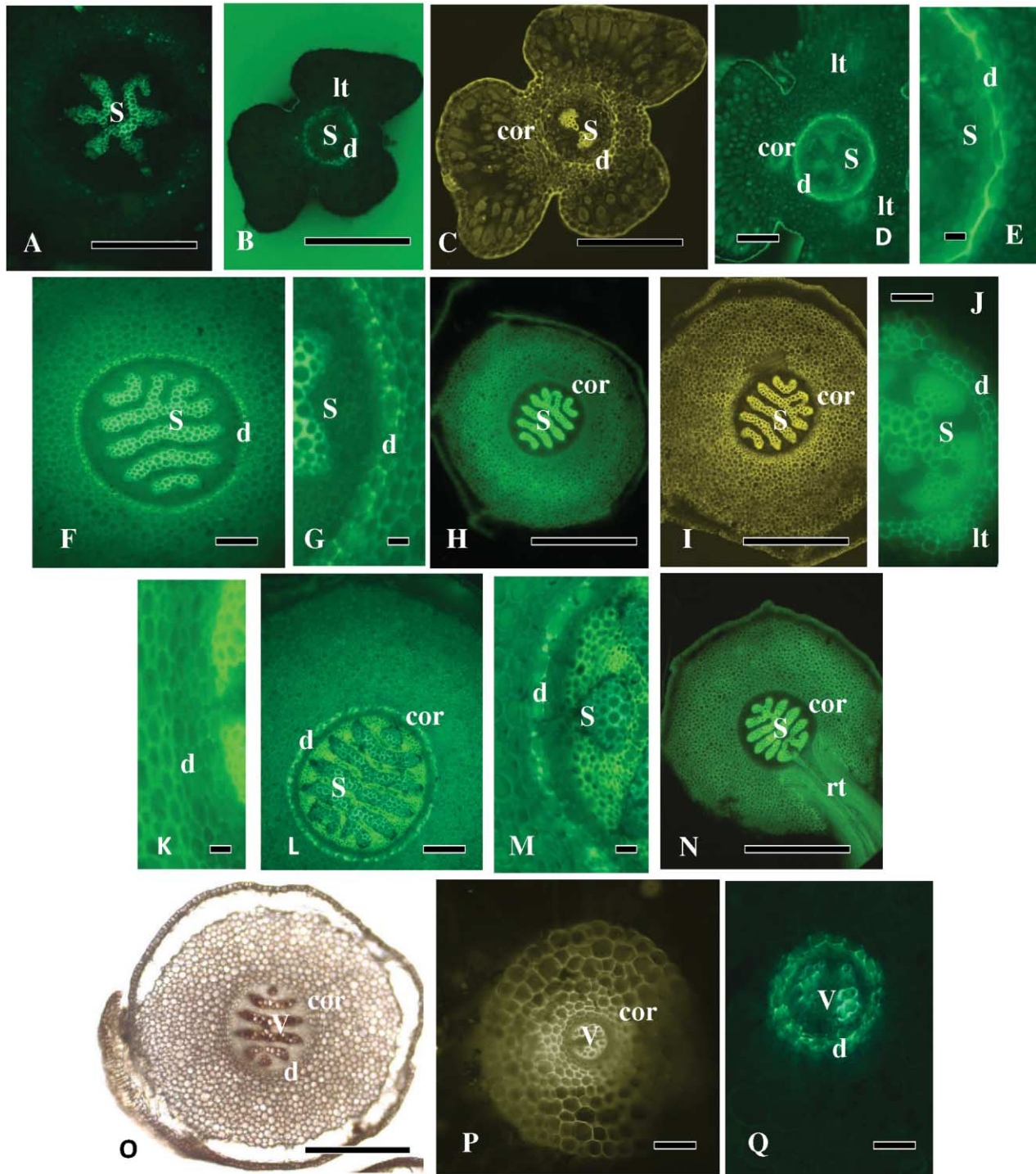


Fig. 3 *Dendrolycopodium obscurum*. *A*, Strobilus axis and no endodermoid, BGVef. Scale bar = 750 μ m. *B*, Stem tip, immature stele, and endodermoid, BGVef. Scale bar = 160 μ m. *C*, Near the stem tip, actinostele, and endodermoid, BGVlc. Scale bar = 350 μ m. *D*, Upper green stem, actinostele, endodermoid, cortex, and microphyll leaf traces, BGVef. Scale bar = 200 μ m. *E*, Upper green stem close-up and endodermoid with thick, wavy walls, BGVef. Scale bar = 100 μ m. *F*, Middle of the green stem, plectostele, and endodermoid, BGVef. Scale bar = 150 μ m. *G*, Close-up of the middle of the green stem, endodermoid, and some Casparian-like bands, BGVef. Scale bar = 30 μ m. *H*, Low green stem, plectosteles, cortex, and no conspicuous endodermoid, UNSTef. Scale bar = 1300 μ m. *I*, Low green stem, plectostele, cortex, and no conspicuous endodermoid, BGVlc. Scale bar = 1000 μ m. *J*, Low green stem, stele, and endodermoid that is present but faint, BGVef. Scale bar = 90 μ m. *K*, Close-up of the rhizome and endodermoid, faint but not strongly stained, FYef. Scale bar = 25 μ m. *L*, Rhizome, stele, cortex, and prominent endodermoid, BGVef. Scale bar = 200 μ m. *M*, Rhizome close-up and endodermoid with some Casparian-like bands, Bef. Scale bar = 40 μ m. *N*, Rhizome, adventitious root perpendicular to the stem stele, and epidermal emergence, BABef. Scale bar = 850 μ m. *O*, Base adventitious root, vascular cylinder-like stem, cortex, and lignified endodermoid, PGbf. Scale bar = 600 μ m. *P*, Adventitious root not exhibiting endodermoid, UNSTef. Scale bar = 140 μ m. *Q*, Distal adventitious root, diarch vascular cylinder, distinct endodermoid, and some Casparian-like bands, BGVef. Scale bar = 50 μ m. See table 1 for definitions of abbreviations.

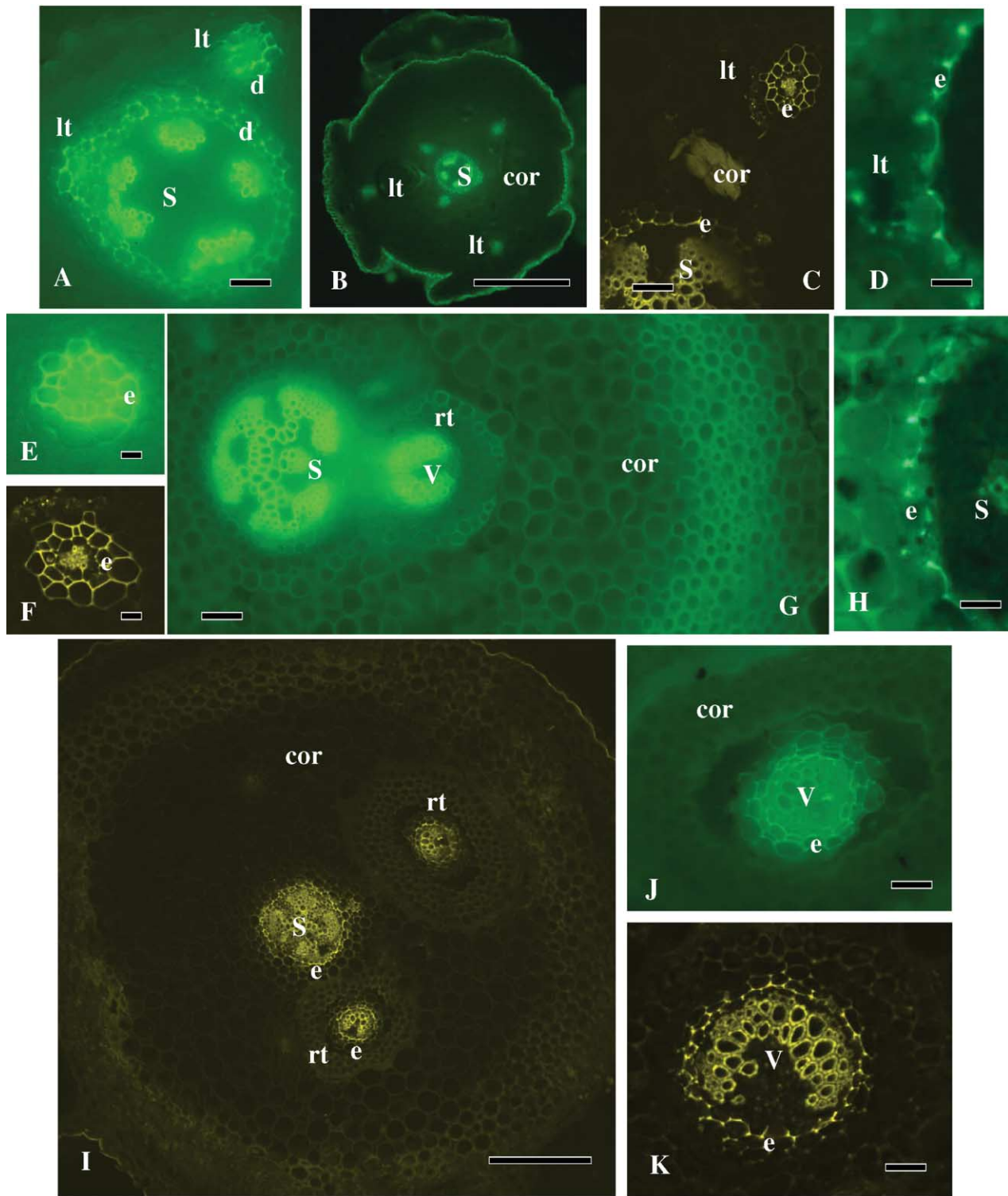


Fig. 4 *Huperzia lucidula*. **A**, Terminal stem near the shoot tip, microphyll leaf traces, and stele endodermoid, BGVef. Scale bar = 220 μ m. **B**, Upper green stem, cortex, and stele microphyll leaf traces, UNSTef. Scale bar = 650 μ m. **C**, Green stem, stele, endodermis, and microphyll leaf trace with endodermis, BGVlc. Scale bar = 120 μ m. **D**, Green stem close-up of stem endodermis with young microphyll leaf trace, BGVef. Scale bar = 45 μ m. **E**, Microphyll leaf trace with endodermis suberized, UNSTef. Scale bar = 40 μ m. **F**, Microphyll leaf trace with endodermis suberized, BGVlc. Scale bar = 40 μ m. **G**, Green stem, stem stele, new adventitious root trace, diarch root vascular cylinder, and endodermis not distinct, Bef. Scale bar = 150 μ m. **H**, Green stem close-up, stem stele, endodermis, and Casparian bands, BGVef. Scale bar = 45 μ m. **I**, Stem base, actinostele with adventitious root trace parallel to the stem axis, microphyll leaf trace with endodermis, and root trace with endodermis, BGVlc. Scale bar = 400 μ m. **J**, Adventitious root trace in stem cortex, vascular cylinder, and endodermis with Casparian bands, BABef. Scale bar = 125 μ m. **K**, Adventitious root trace in stem cortex, diarch vascular cylinder, endodermis with Casparian bands, and some suberin lamellae, BGVlc. Scale bar = 100 μ m. See table 1 for definitions of abbreviations.

epifluorescence), with a relatively small stele internal to a broad cortex and microphyll leaf traces. Lower in the green stem, the innermost region of cortex became an endodermis around a microphyll leaf trace and stem stele, as shown by berberine gentian violet laser confocal microscopy (fig. 4C) and epifluorescence (fig. 4D). Microphyll leaf traces developed an endodermis with evident radial and tangential cell walls, sometimes with slightly overlapping cells, as shown under unstained epifluorescence (fig. 4E) and berberine gentian violet epifluorescence (fig. 4F); these cells had lignin and suberin in their walls. Casparian bands were not conspicuous in steles and root traces stained and viewed in berberine epifluorescence (fig. 4G), but mid-green stem steles had distinct Casparian bands under berberine gentian violet epifluorescence (fig. 4H). Adventitious root traces arose from the stele and descended the cortex parallel to the stele (fig. 4G, 4I), exiting stem bases with a cortical emergence. In adventitious roots at the base of stems, the endodermis was conspicuous (fig. 4I–4K), although it could be seen better with berberine gentian violet laser confocal microscopy (fig. 4K; even with suberin) than with berberine aniline blue epifluorescence (fig. 4J). All adventitious root traces were diarch and developed distinct endodermis (fig. 4G, 4I–4K); the diarch protoxylem poles of the vascular cylinder pointed away from the stem stele (fig. 6G, 6I). Mostly under berberine epifluorescence (fig. 4G) and only slightly under berberine gentian violet laser confocal microscopy, outer cortical cells had thicker cell walls in the stems and roots.

Phlegmariurus squarrosus. The stele of its upright, vertical stem was a complex plectostele (fig. 5A–5G). Near its tip, the stem stele and microphyll leaf traces were encircled by an endodermoid without distinct Casparian bands (fig. 5A); below this, the stem had an endodermis (fig. 5B–5F) in microphyll leaf traces (fig. 5B, 5G, 5H) and adventitious root traces (fig. 5E, 5G). There were clear connections between the stele endodermis and microphyll leaf trace endodermis (fig. 5B). While microphyll leaf traces had an endodermis (fig. 5H), microphylls did not (fig. 5G). The lower stem can have many root traces arising from the stele and descending the cortex (fig. 5G), and there were clear continuities between the stem stele endodermis (fig. 5E, 5F) and the adventitious root trace endodermis with distinct Casparian bands (fig. 5E, 5F, 5I–5K), which were revealed with various staining and microscopic procedures (berberine aniline blue and toluidine blue O epifluorescence and berberine gentian violet and unstained laser confocal microscopy), but especially with berberine gentian violet epifluorescence (fig. 5E, 5F). Adventitious roots often developed suberin lamellae (fig. 5K, 5L). Root vascular cylinders were mostly diarch (fig. 5E, 5G, 5J), except for minor differences (e.g., fig. 5I) probably related to the maturation, amount, and positions of protoxylem; protoxylem poles pointed away from the stem stele (fig. 5E, 5G). Adventitious roots had a cortical emergence from the stem bases. No cortical cell wall thickenings were evident in the stems or adventitious roots.

Selaginellaceae. We examined stems, rhizophores, and roots of select Selaginellaceae; we observed few leaf traces or microphylls without special cells around traces or veins.

Selaginella borealis. In our *S. borealis* plants, stems were usually polystelic, with two or three meristemes (fig. 6A), but monostely occurred (fig. 6B), especially in younger stems. An endodermis, endodermoid, or stele-cortex wall around the steles could not be easily demonstrated with berberine gentian violet epifluorescence (fig. 6A), differential interference contrast (fig. 6B),

berberine aniline blue, unstained specimens, or fluorol yellow epifluorescence (not shown). A stele-cortex wall lining the outer stele cells and inner cortex trabecular cells was only faintly demonstrated in the upper stems; it was not revealed by either Sudan IV or Sudan red 7B bright-field microscopy, and it was well differentiated as an undulating cell wall layer without discernible Casparian bands only with laser confocal microscopy (fig. 6C, 6D). An epidermal cuticle was seen in fluorescence images (fig. 6E), and in 488-nm laser confocal images, it was similar to the stele-cortex wall (cf. fig. 6D, 6E). A few parts of the stele-cortex wall have connections to trabecula cell bases (fig. 6D). Rhizophores emerge at nodes via epidermal emergence in all species; proximal rhizophores of *S. borealis* that we sectioned were unusual in that the vascular cylinder shape was very similar to that of monostelic stems, except that the rhizophores had root hairs but no obvious endodermis (fig. 6F). Most roots (fig. 7G–7I), produced after dichotomies of the rhizophore, normally had a monarch vascular cylinder, an endodermis with Casparian bands in many cells (e.g., fig. 6G–6I), suberin lamellae in some cells (fig. 6I), and root hairs (fig. 6G). Some stems (fig. 6A) and dichotomized roots (fig. 6G, 6H) exhibited sclerenchyma, especially in the outer cortex.

In *Selaginella kraussiana*, stems were polystelic, with two meristemes, in both unstained epifluorescence (fig. 6J) and berberine aniline blue laser confocal microscopy (fig. 6K) images. Each meristeme was surrounded by a ring of cells and a stele-cortex wall (fig. 6J, 6K, 6M, 6N), and there was a distinct epidermal cuticle (fig. 6K) that showed more brightly than the stele-cortex wall in both epifluorescence and laser confocal images. Such meristemes were characterized by the ring or cylinder of stele-cortex wall around each meristeme, without an endodermis with Casparian bands (fig. 6M, 6N). The interruptions in the ring at the stele-cortex wall (fig. 6M, 6N) are places where the tangential cell wall materials flared out into trabecular cells. However, under modified differential interference contrast microscopy, trabecula cells had dark areas that appeared Casparian band-like (fig. 6L). Rhizophores had an endodermis and an epidermal cuticle (fig. 6O, 6P), and the vascular cylinder was protostelic. Dichotomized roots from rhizophores had monarch vascular cylinders and endodermis (fig. 6Q). Small roots (fig. 6R) were distinctly monarch, with an endodermis; suberin lamellae could be found, especially on outer tangential walls (fig. 6Q, 6R). We found no thickened cell wall regions in the mid-outer cortices of stems or roots.

Except where there was a branch (fig. 7A), stems of *Selaginella moellendorffii* had a monostele (fig. 7B–7E). We did not find a brightly stained layer surrounding the stele in any of the epifluorescence procedures (e.g., fig. 7A, 7B), but a very light stele-cortex wall could be seen in some unstained, berberine (fig. 7A), and berberine aniline blue epifluorescence specimens. There was no such wall in berberine gentian violet (fig. 7B) or fluorol yellow epifluorescence specimens (not shown). A faint stele-cortex wall layer could be detected in unstained differential interference contrast specimens (fig. 7C) and some bright-field specimens; the epidermal cuticle fluoresced in modified Sudan IV differential interference contrast when the stele-cortex wall did not (fig. 7D), and trabeculae revealed no obvious Casparian bands (fig. 7D). However, under various treatments with laser confocal microscopy, the stele-cortex wall layer could be seen (e.g., fig. 7E; in berberine gentian violet, Sudan IV [not shown], and berberine toluidine blue O laser confocal microscopy [not shown]); this stele-cortex

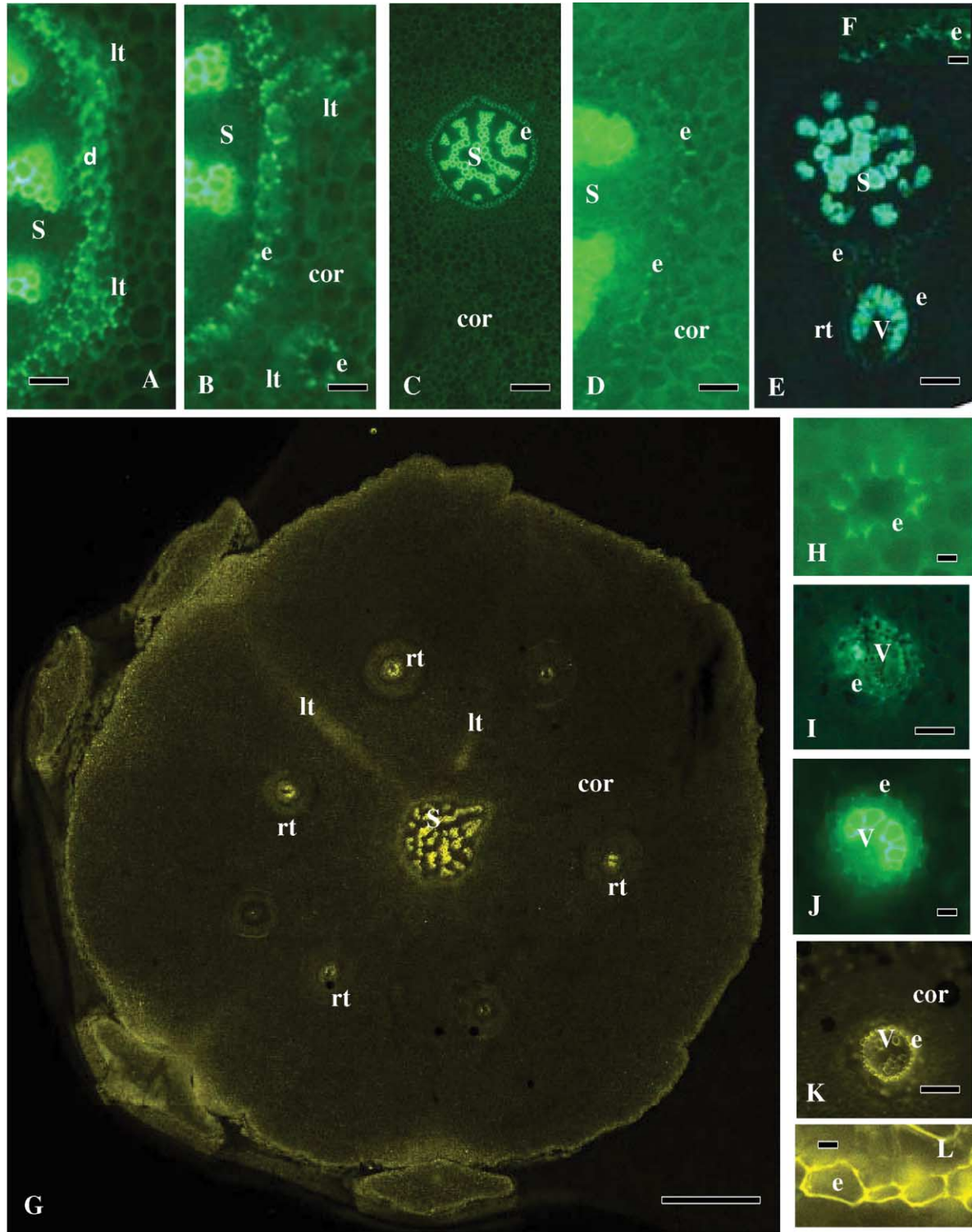


Fig. 5 *Phlegmariurus squarrosus*. **A**, Stem near the tip, stele and microphyll leaf traces with endodermoid, and no obvious Casparian bands, BGVef. Scale bar = 75 μ m. **B**, Upper green stem, stele and microphyll leaf traces with endodermis, and Casparian bands mostly evident, BGVef. Scale bar = 75 μ m. **C**, Upper green stem, cortex, and plectostele with endodermis, BGVef. Scale bar = 225 μ m. **D**, Green stem, edge of stele, cortex, and endodermis with some visible Casparian bands, BABef. Scale bar = 60 μ m. **E**, Stem stele and diarch adventitious root trace, both surrounded by and connected by endodermis, BGVef. Scale bar = 100 μ m. **F**, Close-up of stem endodermis with Casparian bands from **E**, BGVef. Scale bar = 30 μ m. **G**, Tile scan of low stem and four microphylls, stem stele, adventitious root traces, and microphyll leaf traces in cortex, BGVlc. Scale bar = 500 μ m. **H**, Microphyll leaf trace endodermis in stem cortex, BGVef. Scale bar = 30 μ m. **I**, Adventitious root trace, immature vascular cylinder, and endodermis, BTBOef. Scale bar = 100 μ m. **J**, Close-up of diarch adventitious root trace and endodermis, BABef. Scale bar = 35 μ m. **K**, Adventitious root trace, vascular cylinder, endodermis with Casparian bands, and suberin lamellae, UNSTlc. Scale bar = 120 μ m. **L**, Close-up of endodermis with suberin lamellae, UNSTlc. Scale bar = 15 μ m. See table 1 for definitions of abbreviations.

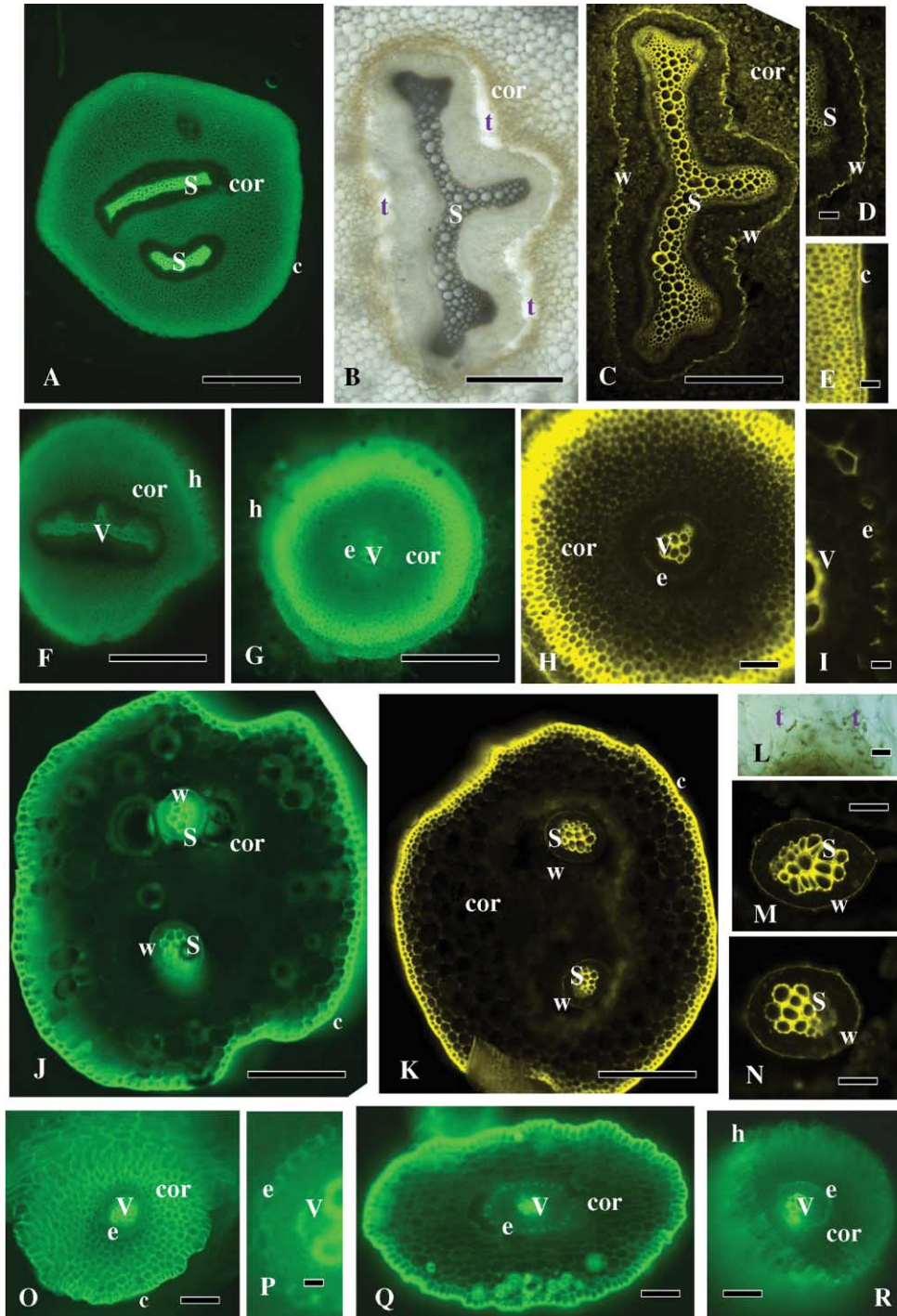


Fig. 6 A–I, *Selaginella borealis*. A, Stem polystele with two meristeles, cortex, and epidermal cuticle, BGVef. Scale bar = 700 μm . B, Low stem, meristele, and trabeculae in lacuna of the innermost cortex, BGVbf. Scale bar = 400 μm . C, Low stem, meristele, and prominent extracellular stele-cortex wall, BGVlc. Scale bar = 360 μm . D, Close-up of stele-cortex wall adjacent to the stele, BGVlc. Scale bar = 60 μm . E, Close-up showing epidermal cuticle, BGVlc. Scale bar = 80 μm . F, Base of rhizophore, vascular cylinder–like stem stele, cortex, and rhizophore hairs, BGVef. Scale bar = 400 μm . G, Dichotomized root beyond the rhizophore, monarch vascular cylinder, cortex, and endodermis, FYef. Scale bar = 375 μm . H, Distal dichotomized root, monarch vascular cylinder, sclerenchymatous outer cortex, and endodermis, BGVlc. Scale bar = 150 μm . I, Close-up of endodermis with Casparian bands and a cell with suberin lamella outside the vascular cylinder, BGVlc. Scale bar = 40 μm . J–R, *Selaginella kraussiana*. J, Stem with two meristeles, cortex, stele-cortex wall, and cuticle, BGVef. Scale bar = 300 μm . K, Stem, two meristeles, cortex, stele-cortex wall, and cuticle, BABlc. Scale bar = 350 μm . L, Close-up of lacuna of the innermost cortex with trabeculae, which are possible Casparian bands, BABdic. Scale bar = 25 μm . M, Close-up of one meristele with an extracellular wall, BABlc. Scale bar = 75 μm . N, Close-up of another meristele with an extracellular wall, BABlc. Scale bar = 75 μm . O, Rhizophore with monarch vascular cylinder cortex and endodermis, UNSTef. Scale bar = 100 μm . P, Close-up of rhizophore, showing part of the vascular cylinder and endodermis, UNSTef. Scale bar = 35 μm . Q, Proximal dichotomized root, cortex, vascular cylinder, and endodermis, UNSTef. Scale bar = 100 μm . R, Distal dichotomized root, cortex, monarch vascular cylinder, and endodermis, UNSTef. Scale bar = 75 μm . See table 1 for definitions of abbreviations.

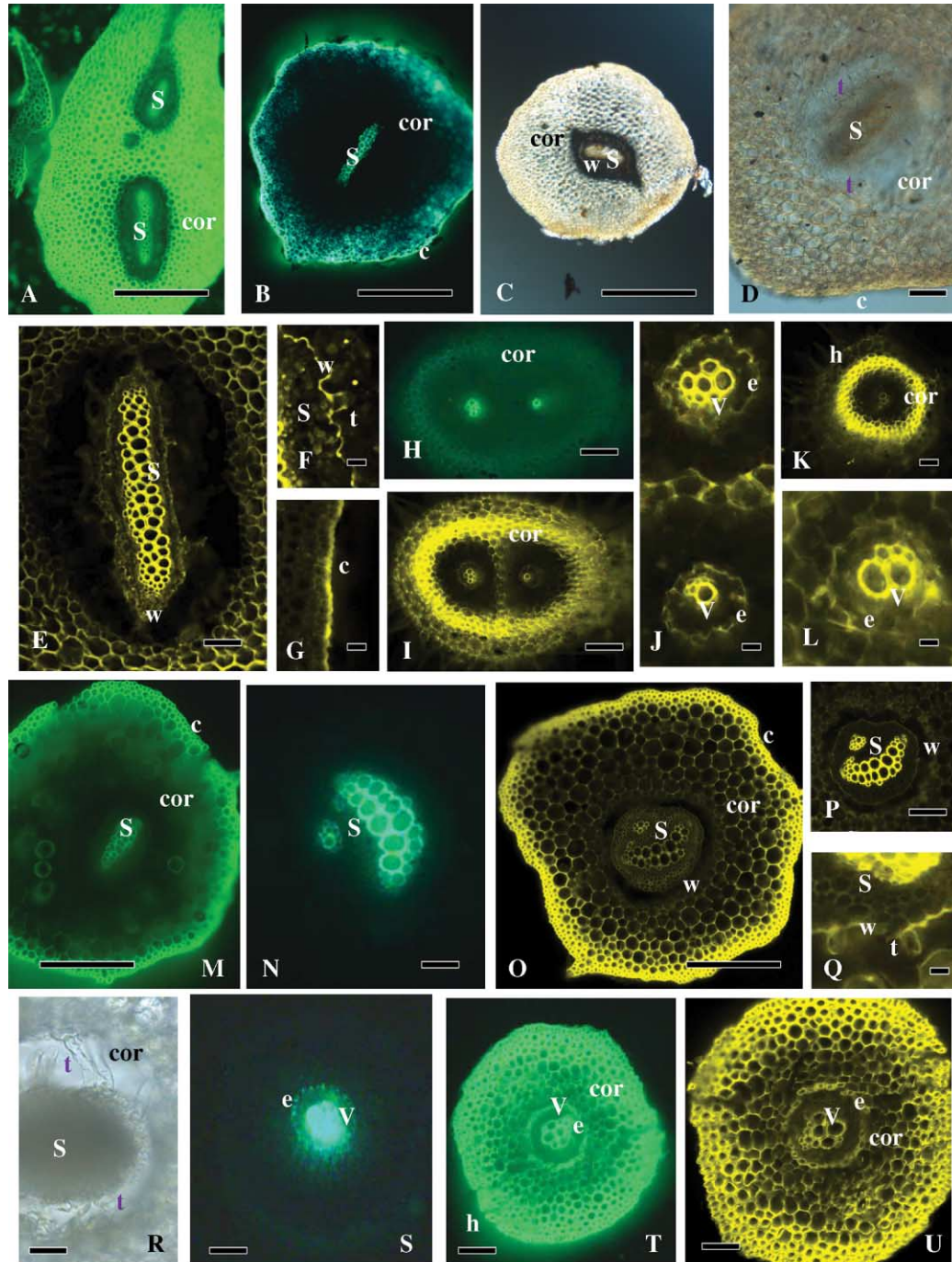


Fig. 7 A–L, *Selaginella moellendorffii*. A, Stem, polystele with two meristele, and cortex, Bef. Scale bar = 400 μ m. B, Stem, monostele, cortex, and no endodermis or stele-cortex wall, BGVef. Scale bar = 450 μ m. C, Stem, monostele, cortex, evidence of a stele-cortex wall, and epidermal cuticle, UNSTdic. Scale bar = 600 μ m. D, Stem, monostele, innermost cortex lacuna with trabeculae, epidermal cuticle, and modified SIVdic. Scale bar = 150 μ m. E, Stem monostele, stele-cortex wall around the stele, and some trabeculae, BGVlc. Scale bar = 90 μ m. F, Close-up of E, with extracellular wall and trabeculae, and stele, BGVlc. Scale bar = 35 μ m. G, Close-up of BGVlc stem and cuticle. Scale bar = 40 μ m. H, Rhizophore dichotomizing with two brightly fluorescing vascular cylinders and cortex, BGVef. Scale bar = 120 μ m. I, Rhizophore dichotomizing with two vascular cylinders and cortex, BGVlc. Scale bar = 110 μ m. J, Close-up of I, endodermis around both vascular cylinders, BGVlc. Scale bar = 40 μ m. K, Dichotomized root, sclerenchymatous cortex, and root hairs, Blc. Scale bar = 100 μ m. L, Close-up of vascular cylinder with endodermis, Blc. Scale bar = 30 μ m. M–U, *Selaginella uncinata*. M, Stem, monostele, cortex, and epidermal cuticle, UNSTef. Scale bar = 600 μ m. N, Stem, typical stele with a large arc of xylem and a small bundle, and no endodermis or endodermoid or stele-cortex wall, BGVef. Scale bar = 60 μ m. O, Stem, typical stele, stele-cortex wall, and cortex, BGVlc. Scale bar = 400 μ m. P, Close-up of the stele in O and stele-cortex wall, BGVlc. Scale bar = 200 μ m. Q, Close-up of the stele-cortex wall with trabeculae, BGVlc. Scale bar = 30 μ m. R, Stem stele, no visible stele-cortex wall, and inner cortex lacuna with trabeculae and without visible wall thickenings like Casparian bands, UNSTdic. Scale bar = 70 μ m. S, Rhizophore, monarch vascular cylinder, and endodermis, BGVef. Scale bar = 80 μ m. T, Dichotomized root, vascular cylinder, sclerenchymatous outer cortex, and endodermis, Bef. Scale bar = 70 μ m. U, Dichotomized root, monarch vascular cylinder, sclerenchymatous outer cortex, and endodermis with Casparian bands and suberin lamellae, Blc. Scale bar = 70 μ m. See table 1 for definitions of abbreviations.

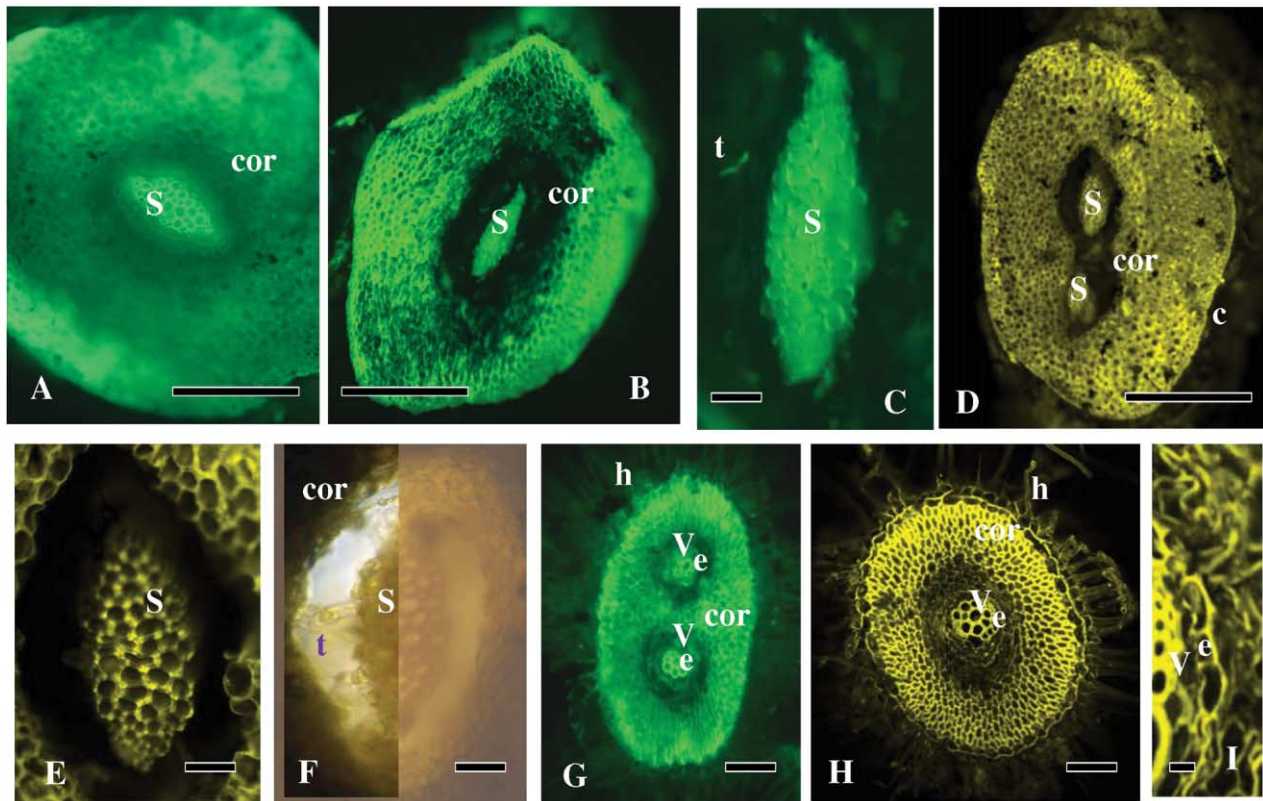


Fig. 8 *Selaginella lepidophylla*. A, Stem 3–4 mm behind the tip, monostele, cortex, and no distinct endodermis or stele-cortex wall, BTBOef. Scale bar = 200 μm . B, Stem 6–8 mm behind the tip, monostele, cortex, and no distinct endodermis or extracellular wall, BGVef. Scale bar = 250 μm . C, Close-up of B, a trabeculae region with two possible Casparian bands, FYef. Scale bar = 70 μm . D, Stem, polystele with two meristemes at the branch, cortex, and no stele-cortex wall, Blc. Scale bar = 350 μm . E, Stem, monostele, and no stele-cortex wall or endodermis, UNSTlc. Scale bar = 70 μm . F, Spliced photos of different foci, stem, monostele, and trabeculae without Casparian bands in the inner cortex lacuna, PGbf. Scale bar = 75 μm . G, Rhizophore at its dichotomy into two roots, rhizophore/root hairs, cortex, and endodermis around both vascular cylinders, Bef. Scale bar = 125 μm . H, Dichotomized root, root hairs, sclerenchymatous cortex, endodermis, and monarch vascular cylinder, Blc. Scale bar = 120 μm . I, Dichotomized root, close-up, vascular cylinder to the left, and endodermis with suberized walls, Blc. Scale bar = 25 μm . See table 1 for definitions of abbreviations.

wall (fig. 7F) contrasted with the stem epidermis cuticle (fig. 7G), which was brighter in the same specimens (cf. fig. 7F, 7G). Undulations or interruptions in the stele-cortex wall usually occurred at trabeculae (fig. 7F). Stems had various regions of thick cell walls in the cortices in various stains. Where the rhizophore dichotomized into adventitious roots, both berberine gentian violet (fig. 7H) and laser confocal (fig. 7I, 7J) images showed small monarch vascular cylinders with few xylem elements but with a distinct endodermis and even suberin lamellae in some cells (fig. 7J). Each adventitious root (fig. 7K, 7L) had a monarch vascular cylinder surrounded by an endodermis with Casparian bands and suberin lamellae on the tangential walls. There was no obvious epidermal cuticle or exodermis (fig. 7K), but many layers of the midcortex were sclerenchymatous (fig. 7I, 7K).

Stems of *Selaginella uncinata* had either a simple monostele with one bundle of xylem (fig. 7M) or, more commonly, a stele with one large, curved bundle accompanied by one small bundle of xylem—mostly protoxylem—opposite the concave arc of the larger bundle (fig. 7N–7P). At the outer edge of the monostele and the inner lining of a lacuna, there was a faint epifluorescence of a stele-cortex wall in fluoro yellow epifluorescence (not shown)

and berberine laser confocal (fig. 7O) images; neither unstained (fig. 7M) nor berberine gentian violet epifluorescence (fig. 7N) specimens revealed a stele-cortex wall. A berberine gentian violet laser confocal–stained stem revealed a stele-cortex wall (fig. 7P, 7Q). In berberine gentian violet laser confocal images, an immediately adjacent stele-cortex wall was continuous with trabecular cells (fig. 7Q); no such wall or cells were evident in berberine gentian violet and berberine aniline blue epifluorescence specimens (e.g., fig. 7N) or in unstained differential interference contrast preparations, although trabeculae were shown clearly (fig. 7R). Sections of a rhizophore revealed a monarch vascular cylinder and an endodermis with Casparian bands in berberine gentian violet epifluorescence (fig. 7S); the roots in berberine epifluorescence (fig. 7T) and laser confocal (fig. 7U) images had a monarch vascular cylinder and an endodermis with Casparian bands and suberin lamellae (fig. 7S–7U). The only regions of the cortex with thicker cell walls were the outermost layers of the stems and roots (fig. 7T, 7U).

Selaginella lepidophylla plants, which we watered to rejuvenate from a desiccated condition to an open shoot position, had no evidence of an endodermis, endodermoid, or stele-cortex

wall around their stem monosteles within 3–4 mm of a stem tip (fig. 8A) or within 6–8 mm of a stem tip (fig. 8B). Outside the stele, there was only very faint evidence of any kind of wall encircling the steles in stem segments in epifluorescence treatments (e.g., fig. 8A [berberine toluidine blue O], 8B, 8C [berberine gentian violet]). A magnified close-up view of the berberine gentian violet epifluorescence specimen (fig. 8C) showed a possibility of two Casparian-like walls or trabeculae. Near the branching stem, a polysteles with two meristeles occurred (fig. 8D). But unlike in other *Selaginella* species (figs. 6, 7), no such stele-cortex walls were evident around the meristeles in laser confocal (fig. 8D [berberine laser confocal microscopy], 8E [unstained laser confocal microscopy]) or in unstained bright-field (fig. 8F) images, even though the epidermal cuticle was evident (fig. 8D). A lacuna was not always apparent in the basalmost stem sections; stained in phloroglucinol bright field, the lignified xylem cells stained red (fig. 8F), but in lacunae, no trabecular cell exhibited lignin. As they arose from the dichotomy of a rhizophore, dichotomized roots (fig. 8G) had small monarch vascular cylinders with an endodermis around the stele and root hairs in berberine epifluorescence images. Proximal roots beyond the dichotomies had monarch vascular cylinders (fig. 8H), and distal roots had very few xylem elements; both had root hairs (fig. 8H) and endodermis with Casparian bands and prominent suberin lamellae in outer tangential walls (fig. 8I). In the position of a cortical exodermis, there was a fluorescent outer tangential wall layer under the epidermal hair cells (fig. 8G); the epidermis (with root hairs) remained a distinct layer surrounding the root, even after prolonged desiccation. Stem and root cortices usually had thicker sclerenchymatous cell walls in various stains and microscopic analyses.

Discussion

Lycopodiaceae. In his recent description of the family with respect to the presence or absence of an endodermis, Stevens (2021) portrayed the Lycopodiaceae as “endodermis 0 [?]”; he must have had the question mark because good, demonstrable photographs of the inner cortex of these lycopods are extremely sparse in the literature. The members of the Lycopodiaceae Lycopodioideae that we studied, *Lycopodiella inundata*, *Lycopodium clavatum*, *Dendrolycopodium obscurum*, and *Diphasiastrum complanatum*, have a unique feature at the boundary between their inner cortices and their stem stele and root vascular cylinder. There is a circumferential zone of cells with variously modified and sometimes quite irregular cell walls that does not fit the definition of a true endodermis with easily demonstrable Casparian bands, although some cells in *D. complanatum* roots and *D. obscurum* stems and roots had a Casparian band-like structure. We have termed this ring an endodermoid, and it appears in various forms in stems and roots. Even the multilayered ring between the primary phloem and most of the inner cortex that stains variously under toluidine blue O bright field or other epifluorescence and laser confocal stains is itself evidence of a cell wall structure and composition different from that of adjacent tissues. In *Huperzia lucidula* and *Phlegmariurus squarrosus*, members of the Huperzioideae, we found that a similar ring of cells in mature stems and roots can be termed an endodermis because the cells exhibit Casparian bands, although it is not certain that they function like typical Casparian bands (Geldner 2013; Meyer and Peterson 2013; Soukup and Tylová 2018).

This unique region of the inner cortex between the conspicuous cortex and stele has long been known and illustrated (summarized by Ogura 1972), mostly in drawings of species of *Lycopodium* stems where a distinct layer of cells in the inner cortex rings the stele like an endodermis (see Sachs 1882, figs. 100, 328). In his article on pteridophytes and gymnosperms, including the Lycopodiales, Jeffrey (1902, p. 134) noted that *L. clavatum* has “no endodermis (phloeoterma) distinguishable,” that *Phylloglossum* has “a tubular central cylinder surrounded by a well marked endodermis,” and that the *H. lucidula* (synonym, *Lycopodium lucidulum*) “endodermis is strikingly present.”

The illustrations of various species of *Lycopodium* (some now *Huperzia* or *Phlegmariurus*) in Jones (1905, pl. 3 [*L. clavatum*] and pl. 3.2 [a drawing with an endodermis label]) reveal the same kind of circumferential zone that we describe as an endodermoid or even endodermis. Hill’s (1919, fig. 1) photograph of *Phlegmariurus reflexus* (synonym, *Lycopodium reflexum*) showed three roots vertically traversing the cortex outside a small stem stele, and each root had a clearly distinct ring around its singular vascular cylinders that would be the endodermis. The drawings of stem and microphyll trace sections by Turner (1924, fig. 6) showed the endodermis around the stele and vein in *H. lucidula* (synonym, *L. lucidulum*); Turner (1924) also noted the endodermis around the vein in 2-yr-old microphylls. The photo of *Lycopodium serratum* by Bierhorst (1971, p. 10, fig. 2-2A; now *H. serrata*) shows a complete thicker-walled layer of innermost cortex that is probably the stem endodermis of *H. serrata*. A photo in Gifford and Foster (1989, fig. 9.5B) showed a distinctly thick-walled ring with apparent suberin lamellae, along with a connected leaf trace around the stele, in *Huperzia selago* (synonym, *Lycopodium selago*). Chu (1974), however, had no evidence of an endodermis around the microphyll veins (see also Bhambe 1965).

The occurrence of an endodermis in roots and stems of members of the Lycopodiaceae has been disputed; Damus et al. (1997, p. 193) did not find any Casparian bands or lignin in such a layer in *L. inundata* (synonym, *Lycopodium inundatum*). However, Damus et al. (1997, figs. 7–9 [*D. obscurum*], 10, 11 [*H. lucidula*]) had illustrations that seemed to show that no such layer was present in *Dendrolycopodium* (synonym, *Lycopodium*) and *Huperzia* (synonym, *Lycopodium*) in the species they reported. But their figures 9 and 11 reveal vascular cylinders with fluorescence that is rather similar to the autofluorescence in their figures 8 and 10, respectively, and without the obvious vascular cylinder fluorescence attributable to the yellow berberine thiocyanate crystals present in apoplastic permeability tests, as in the epidermis and cortex of those roots. We believe that there is an endodermoid in *Dendrolycopodium* and endodermis in *Huperzia*, by the definition of Geldner (2013), but whether or not the cell wall materials—that is, the types of lignin and suberin—are sufficient for the endodermoid cell walls of *D. obscurum* or the endodermal Casparian bands of *H. lucidula* to prevent water and mineral movement through the cell walls is in question. In *P. squarrosus*, Casparian bands are even more prominent around both the stem stele and root vascular cylinders within the stem cortex.

Arana et al. (2014, fig. 1E [microphyll], 1H [stem], 1J [stem with a leaf trace]) labeled an endodermis in *Phlegmariurus phyllicifolius* organs; only in their figure 1H did those cells have slightly thickened inner tangential walls around the stem stele, which directly abutted the pericycle in *P. phyllicifolius*. But they were not

thickened in a leaf trace under traditional hematoxylin-safranin-stained bright-field microscopy, and Casparian bands could not be seen. Kessler (2009, figs. 18, 19) had light micrographs of *Huperzia mandiocana* showing a ring of cells around the stem stele, supposedly with U-shaped walls, but no Casparian bands were evident. Kessler (2009, figs. 31–34) also demonstrated the inner tangential walls of an endodermis with Sudan IV and phloroglucinol bright-field microscopy of the roots, but he revealed no Casparian bands. Pita et al. (2006, figs. 15, 16) photographed an endodermis with stained walls around the cells and lightly stained walls around the leaf traces of *Huperzia friburgensis*, but not around the single vein in the microphylls. Our illustrations of root traces of members of the Huperziaceae demonstrate Casparian bands in an endodermis; the singular stele in the stems of these plants also shows an endodermis. Otherwise, members of Lycopodiaceae have been studied little for endodermis Casparian bands, except by Damus et al. (1997).

The origin of adventitious roots that are perpendicular to the stem stele via epidermal emergence has long been illustrated among the Lycopodiaceae (e.g., *D. complanatum* by Wigglesworth [1907, figs. 10–12] and Roberts and Herty [1934, pl. 2]). In Huperziaceae, Stokey (1907, figs. 2, 15) illustrated *Phlegmariurus pithyoides* (synonym, *Lycopodium pithyoides*), and then Hill (1919, fig. 1) drew adventitious roots of *P. reflexus* (synonym, *L. reflexum*), which arise from the stele and grow vertically down or parallel to the stele through the stem cortex to the rhizosphere; they have been known to have a cortical emergence. The origin of these adventitious roots as diarch, growing vertically in the stem cortex, was shown for *H. serrata* (synonym, *Lycopodium serrata*) in drawings by Stokey (1907, fig. 12) and Hill (1919, fig. 1) and in photomicrographs by Bierhorst (1971, fig. 2-2A). The position of such cortical roots in *H. selago* (synonym, *L. selago*) was also shown by Gifford and Foster (1989, fig. 9.5A). More recently, Kessler (2009, figs. 23, 25, 26) showed numerous root traces in the cortex of stems of *H. mandiocana*. We did not observe the sclerenchymatous outer cortex of such roots, as shown by Stokey (1907) and Bierhorst (1971). We also did not observe the apical origin of such roots, as drawn by Bruchmann (1874) and Kaplan (2022) for *L. inundata*; no roots that we observed arose at the stem tips, as they arose from the periphery of the stem stele in midlength stems or lower.

The position of the origin and emergence of the adventitious roots of the lycopods have been noted to be an “absence of cortical root emergence” in Lycopodiaceae versus a “cortical emergence of roots” in Huperziaceae (Field et al. 2016, p. 642) or “root emergence non-cortical” as opposed to “root emergence cortical” (Field et al. 2016, p. 652). While all adventitious roots grow through the stem cortex in these plants, we conclude that the origin of the adventitious roots of Lycopodiaceae is best described as an epidermal emergence because these roots grow perpendicularly from the stele across the cortex to emerge through the epidermis opposite their point of origin, which is very common among plants. It is interesting that, in the species studied herein, the Lycopodiaceae with epidermal emergence do not have a well-defined endodermis, even in their roots, but the Huperziaceae with a cortical emergence develop an endodermis. This was described or drawn for lycopods by Stokey (1907) and Wigglesworth (1907, figs. 3, 5, 9, 10, 12–13, 17), who labeled a distinctive layer around the root vascular cylinder a “protective sheath” for the Lycopodiaceae *D. complanatum* (Wigglesworth

1907) and an “endodermis” for the Huperziaceae *Phylloglossum drummondii* (Wigglesworth 1907, e.g., fig. 20). But no such label was given for *L. clavatum* (Wigglesworth 1907, fig. 4). Stokey (1907), Bierhorst (1971), and Kessler (2009) also illustrated sclerenchyma in the outer root cortex. In the basalmost member of the Huperziaceae (Field et al. 2016), Bower (1885, p. 678, fig. 41) had noted only an “ill-defined bundle sheath” around the vascular tissues in roots of the tuberous *Phylloglossum* but nothing in the tubers; Wernham (1910, p. 338) noted an endodermis around a monarch vascular cylinder in roots but no endodermis in stems.

An interesting difference between members of the Lycopodiaceae and Huperziaceae is that Lycopodiaceae have zones of thick-walled stem cortex immediately adjacent to the endodermis (and some in the outer cortex), whereas Huperziaceae do not, except for apparent cellulosic thickened cells in the outer cortical zone in some specimens of *H. lucidula*. This undoubtedly relates to the passage of adventitious roots parallel to the stele and vertically through the cortex for cortical emergence in Huperziaceae.

The occurrence of mycorrhizae, while much investigated in lycopods, can reveal interesting support for our finding of an endodermis in *Huperzia*. For example, Winther and Friedman (2008, p. 795, fig. 3b–3d) have photos of an apparent endodermis with modified cell walls in *Huperzia hypogaea* roots, in which mycorrhizae occur “predominantly within the large cortical parenchyma cells that surround the vascular cylinder” (Winther and Friedman 2008, p. 793), but not the innermost layer of cortex, the endodermis (unlabeled), or the cells of the vascular cylinder. The presence of an endodermis with Casparian bands (and suberin lamellae) would allow for this exclusion of mycorrhizae from the endodermis and vascular cylinder. Hoysted et al. (2020, fig. 1g) present SEM of a root of *L. inundata* in which mycorrhizal fungi occupy cells through the cortex into the edge of xylem; this indicates that there is no endodermis blocking mycorrhizal fungi from colonization of the roots.

Selaginellaceae. Stevens (2021) recently described the cortex of the Selaginellaceae as “hypodermis suberized/with Casparian strip; stele in central cavity surrounded by trabeculate endodermal cells.” This is long after Harvey-Gibson (especially 1894, 1897, 1902), Webster and Steeves (1963, 1964, 1967), and Webster and Jagels (1977) conducted detailed stem and root analyses of various *Selaginella* species and reported an endodermis in *Selaginella*, but without photos demonstrating it. Buck and Lucansky (1976, p. 12, figs. 5, 6) noted “trabeculae comprised of a single endodermal cell” plus more cortical cells, but this was not manifested in their photographs. Examining the basalmost member of the Selaginellaceae, *Selaginella selaginoides*, Karris (1981, p. 249, figs. 11, 14, 20) stated that a root endodermis, initially with only Casparian bands and later with suberin, was connected to a hypocotyl endodermis, but an endodermis with Casparian bands was “too small and lightly stained to be seen.” The photographs looked much like our endodermis in Lycopodiaceae; there is no rhizophore in *S. selaginoides* (Weststrand and Korall 2016).

Unlike the bases of the rhizophore of *Selaginella borealis* in our study, its dichotomized roots and the rhizophores and roots of other *Selaginella* species we studied have an endodermis around a monarch vascular cylinder (see also Imaichi and Kato 1989, fig. 1B, without an obvious endodermis). In 1997 Damus

et al. (1997, figs. 4, 6, 12, 15–17) used fluorescence to photograph roots of *Selaginella uncinata*, *Selaginella pallescens*, and *Selaginella kraussiana* with an endodermis and chromic acid digestion to photograph roots of *S. selaginoides* and *S. kraussiana* with an endodermis. Photographs in Schulz et al. (2010, fig. 2G, 2L, 2M) did not reveal an endodermis or Casparian bands in *Selaginella apoda* rhizophores or roots.

In their photos of *S. apoda* stems, Schulz et al. (2010, fig. 1K, 1L) labeled a Casparian band in the middle trabecular cells that could just as easily be on the exterior of the cells and be cuticle or suberin, not lignin; the pericycle in their figure 1K–1M could just as easily be the innermost cell wall layer of the inner cortex (see Ogura 1972). However, Schulz et al.'s (2010) figure 1I reveals a distinct pericyclic layer adjacent to the primary phloem and cells aligned directly with the trabeculae, but without Casparian bands.

Among the other Selaginellaceae, adequate illustrations of the stem endodermis have been rare; Gola and Jernstedt (2016, fig. 2c [1–3]) presented the most interesting dilemma of endodermis identity when they showed an almost uninterrupted, uneven, autofluorescing ring around each “meristele” or singular monostele in *S. kraussiana*. For their bright-field clearing photos, Gola and Jernstedt (2016, p. 4, fig. 1b, 1c) state that “each meristele was enclosed in its own endodermis, the short trabeculae with Casparian strips,” which they labeled “trabecular rings” (not Casparian bands or endodermis). Such trabecular rings or Casparian bands are not visible in their other figures (Gola and Jernstedt 2016, p. 5, figs. 1d, 2b [1–11]). However, their figures are somewhat similar to our images of trabeculae in figures 6B, 6L, 7D, 7R, and 8F. Their propidium iodide–stained fluorescent and UV autofluorescent micrographs (Gola and Jernstedt 2016, fig. 2c) reveal no cells with Casparian bands (except for two bright spots in fig. 2c [2], the right meristele, but those may be involutions or corners of walls), as one might expect on the basis of Damus et al. (1997, figs. 4, 6, 12, 15–17). Their image in figure 2c (3) is more similar to our laser confocal images (figs. 6C, 6D, 6M, 6N, 7E, 7F, 7Q), with bright stele-cortex walls and trabeculae. If one compares the photos in Gola and Jernstedt (2016; cf. fig. 2b [1–11] and 2c [1–3]), the trabeculae clearly do not completely encircle the steles, presumed Casparian bands are located on cell walls adjacent to air spaces of the lacuna, and the thickenings on trabecular cell walls extend to the stele end of the cells (see figs. 6C, 6D, 6M, 6N, 7E, 7F, 7Q). Gola and Jernstedt (2016, p. 9) state that “the presence of Casparian strips [17], additionally encircled by trabecular rings [22]” means that their “results are consistent” with the usual functional role of the endodermis and trabeculae but also that trabecular rings are not Casparian bands. Thus, there is a question about which cells make up an endodermis because it is highly unlikely that the cells shown in Gola and Jernstedt (2016, cf. figs. 1c, 2c) could have fluoresced to produce the rings. In other words, Gola and Jernstedt's figure 2c (3) reveals a structure like our stele-cortex wall, with that wall bordering the stele and trabecular cells; it is not an endodermis of a continuous layer of cells adjacent to a pericycle. The “trabecular ring” in McLean and Juniper (1979, p. 444, figs. 1, 2, 4, 6, 9) is separate from the Casparian band in their study of *S. kraussiana*.

Images in Grego-Valencia et al. (2018, figs. 2D, 2D', 4A, 4B, 4B') appear to show Casparian bands, but these could be on the exterior of the cells, and they do not appear in their figure 2A

and 2C. In Grego-Valencia et al. (2018, fig. 2A, 2C), any difference between the pericycle and trabecular cells is also unclear. Suganya et al. (2011, pl. III, figs. d, j) revealed a slightly thickened wall layer around the stele at the base of the trabeculae but no Casparian bands in the trabeculae at all. These clearly suggest that the slightly thicker cell walls ringing the steles in other studies are not pericycle or endodermis cells but are an extracellular ring of cell wall material on the surface of the cells outside the primary cell wall. Such a thickened cell wall layer in *S. apoda* shows only as a white layer that Schulz et al. (2010, p. 696, fig. 1K, 1L) describe as “a trabecular ring (= Casparian strip; arrow).” Cardoso et al. (2020, p. 10, fig. 5b, 5d, 5f) have photos of *Selaginella haematodes* and *Selaginella pulcherrima* that do not reveal Casparian bands in “lignin autofluorescence” under UV light; they label an endodermis with some thickened cell walls but no obvious Casparian bands and no extracellular walls under fluorescence or bright-field microscopy. The expression “trabecular ring” leaves some ambiguity about its meaning and the structures.

In 1920, Uphof associated cell wall thickening, especially suberin, in *Selaginella* species with growth in arid environments. As shown and discussed by many (see Meyer and Peterson 2013), a cortical exodermis, where the epidermis has been lost, functions with its suberin lamellae, as might be suggested for an inner cortical cell wall layer ringing the edge of the stele. In our *Selaginella* species with stele-cortex walls, an epidermal cuticle is prominently present. Ogura (1972 and references cited) made the point that the trabecular cells in the lacunae are part of the inner cortex and do not represent an endodermis or pericycle; thus, the trabecular cells with apparent Casparian bands are not endodermis, or they may not have the chemical constituents typical and necessary for endodermis (see Schreiber 1996; Schreiber et al. 1999; Schreiber and Franke 2011; Soukup and Tylová 2018). These cells do not have typical fluorescing Casparian bands like most vascular plant species. One trabecula or multiple trabeculae traversing a lacuna should not be termed an endodermis if there is only one cell per trabecula with apparent Casparian bands. If the trabecular cells with Casparian bands were a continuous layer of cells early in the development and expansion of the zone where a lacuna forms, then that layer or ring of cells might be an endodermis, but such evidence has not been produced. The photo of *Selaginella lepidophylla* in Rafsanjani et al. (2015, fig. 1e) shows only a partial lacuna and no strongly imaged thick cell walls or Casparian bands in a zone around the stele under toluidine blue O staining. Suganya et al. (2011, pl. III, fig. j) clearly demonstrated a ring in the position of the endodermis in *Selaginella tenera*, but there is no mention of the technique used, and it was not similar to the epidermis cuticle in other photos.

Development. The foregoing raises issues of the origin of the innermost cortex and outermost stele in the lycophytes, especially *Selaginella*. The development of a single layer of ground meristem cells to become endodermis is usually very precise and distinctive in the roots, especially in angiosperms, from which most knowledge is derived (e.g., Pauluzzi et al. 2012; also Seago and Marsh 1989; Heimsch and Seago 2008), except in roots that have common initials where the boundary between procambium and ground meristem (thus, the proendodermis) becomes clearer at the proximal edge of the common initials. The boundary in lycophyte photos is not nearly so distinct. Textbook photos of lycophyte shoot and root apices with apical cells illustrate how difficult it is to distinguish between the procambium and inner ground

meristem (e.g., for roots: *Lycopodium* [Steeves and Sussex 1989, fig. 13.11]; for shoots: *Lycopodium* [Gifford and Foster 1989, fig. 9.7a, 9.10a] and *Selaginella* [Gifford and Foster 1989, fig. 9.23, 9.25; Lux et al. 2017, fig. 61]). In research articles on lycopods, photographs of meristematic Lycopodiaceae (roots: e.g., Fujinami et al. 2017, figs. 1, 2 [*L. clavatum*, *D. complanatum*, *L. inundata*, *D. obscurum*, and *Huperzia* species]; Fujinami et al. 2021, fig. 1 [*L. clavatum*]; e.g., for shoots: Gola and Jernstedt 2011 [*H. lucidula*]; Fujinami et al. 2020, fig. 2 [*L. clavatum*]; Evkaikina et al. 2017, figs. 1, 6 [*H. selago*]) and Selaginellaceae (rhizophores: e.g., Imaichi and Kato 1989, fig. 4 [*S. uncinata*]; Lu and Jernstedt 1996, figs. 5, 7 [*S. martensii*]; Otręba and Gola 2011, figs. 2, 4 [*S. kraussiana*]; roots: Imaichi and Kato 1989, fig. 6 [*S. uncinata*]; Fujinami et al. 2017, figs. 4c, 5; Lu and Jernstedt 1996, fig. 7 [*S. martensii*]) do not show a clear boundary between the procambium and ground meristem. All of this may partially explain the variations in the ring of tissue surrounding any stem steles or root vascular cylinders and why it is so difficult to obtain images of an endodermis, endodermoid, or stele-cortex wall—the cells of this zone are irregular in their origins, organizations, and chemicals. The Gola and Jernstedt (2011) study, in particular, demonstrates how changes in apical cells of *H. lucidula* might lead from an endodermoid in the stem tips to an endodermis in the mature lower stems. Another complicating factor in stems with numerous microphylls is that the origins of microphylls would make it inevitable that an endodermoid or endodermis would be uneven and more than one cell thick in places.

Furthermore, examinations of the illustrations of the Lycopodiaceae (Stevenson 1976 [*H. lucidula*]; Pita et al. 2006 [*Huperzia heterocarpon*]; Kessler 2009 [*H. mandiocana*]; Fujinami et al. 2017, 2020 [*H. lucidula*]) and Selaginellaceae (e.g., Stevenson 1976; Imaichi et al. 2019 [*H. lucidula*]; McLean and Juniper 1979 [*S. kraussiana*]; Jacobs 1988 [*Selaginella rupestris*]; Imaichi and Kato 1989 [*S. uncinata*]; Gifford and Foster 1989 [*S. kraussiana*]; Imaichi and Hiratsuka 2007 [multiple species]; Otręba and Gola 2011 [*S. kraussiana*]) illustrate the difficulty in separating the development of any pericyclic layer and endodermal layer in the shoots or even roots of these plants because early in differentiation, they always appear to overlap or have common precursors, in spite of the drawings in Ogura (1972, fig. 150), Gifford and Foster (1989, fig. 9.24 [*Selaginella sinensis*]), and Fujinami et al. (2017, figs. 1, 2, 5), which show boundaries between the stele and cortex with a singular innermost layer in *Lycopodium* roots. But none has shown the developmental association between meristem and primary tissues.

Hence, the origin of the tissues making up the innermost cortex and outermost stele of the lycopods has long been a dilemma (see “Introduction”). For example, Bierhorst (1971 [*Lycopodium samoanum*]), Stevenson (1976 [*H. lucidula*]), Fujinami et al. (2017, 2021 [*H. lucidula*]), Pita et al. (2006 [*H. heterocarpon*]), and Kessler (2009 [*H. mandiocana*]) have demonstrated various modifications in developmental stages among the Lycopodiaceae, but none has shown a convincing association with the stem apical cell or cells.

In his detailed drawings of *Selaginella*, Barclay (1931, p. 461, figs. 1, 2) illustrated that the pericycle and endodermis, in the form of trabeculae with Casparian bands, had a common origin: “Endodermis, pericycle, and vascular strand have a common origin and are all stelar. The endodermis forms the outer layer of the stele.” Yet Barclay (1931, p. 456) stated under the heading “Cor-

tex” that “increase of internal diameter of the cortical cylinder, together with its growth in length, brings about the formation of air cavities and the separation and stretching of the endodermal cells.” Barclay (1931, figs. 1–4) had no photomicrographs to confirm his claims in drawings. We find that Barclay’s drawings without photographic evidence lead to the conclusion that it is the inner cortex and outer stele that have a common origin. Photos and diagrams in Gifford and Foster (1989, cf. fig. 9.23–9.25) show the difficulty in interpreting shoot cell files at their origins in the stele and cortex.

In the images of shoot apices from Dengler (1983, figs. 6, 7), Jacobs (1988, figs. 1–5), Harrison et al. (2007, figs. 4, 6), and Vasco et al. (2016, fig. 3), there is no good demonstration of the development of tissues that would corroborate Barclay’s (1931) conclusion or Ogura’s (1972) and McLean and Juniper’s (1979) claims about *Selaginella*. Schulz et al. (2010, pp. 696, 699, fig. 1K, 1L) labeled clear lines in cells as “trabecular rings (= Casparian strip, arrow).” They found “one endodermal cell” in each trabecula and stated that the outer cell layer of the stele was a pericycle (Schulz et al. 2010, p. 699); their figure 1I image is the single best illustration that a pericycle immediately adjacent to the primary phloem is the outermost layer of a stele. Gola and Jernstedt (2016, p. 6, fig. 1c) photographed trabeculae with two dark lines in one trabecular cell and stated that “each meristele was . . . in its own endodermis, the short trabeculae with Casparian strips on transverse and radial walls.” These were not especially obvious in their figure 1b, and the staining methods for these sections are not stated—unlike those for figures 2c (1), 2, and 3, in which the rings strongly resemble our stele-cortex wall, not an endodermis. Images in Brulé et al. (2019, fig. 3; immunofluorescence) that show lignified cell walls of the stele xylem and sclerenchymatous outer cortex do not show any lignified cells in the lacuna of *S. lepidophylla*.

As noted above, this is complicated by the claims, starting with Harvey-Gibson (1894, 1896, 1897) and shown by McLean and Juniper (1979, fig. 3, at three arrows and on some trabecular cell walls), that a cuticle is present. Grego-Valencia et al. (2018; cf. figs. 2A, 2C, 2D, 2D’ [showing Casparian bands safranin–fast green stained in bright field], 4A–4C [electron microscopic images]) showed that the outer tangential walls of the pericycle and some locations along the trabeculae in *S. pallescens* (fig. 4A, 4B, 4B’) had a cuticle, presumably cutin, but the histochemical evidence in Grego-Valencia et al. (2018, fig. 2A, 2C, 2D, 2D’) is lacking. Their figure 4B shows an apparent Casparian band in a pericycle labeled as a cell, not in the trabecular cell with the labeled cuticle. In both McLean and Juniper (1979) and Grego-Valencia et al. (2018), the base of the trabeculae could be part of the so-called pericyclic layer, and the extra wall material could be cutin or suberin. There might be Casparian bands, but without the kinds of lignins to make them functional Casparian bands, per Schreiber (1996), Enstone et al. (2003), Novo-Uzal et al. (2012), and Soukup and Tylová (2018). It should be noted that in *S. uncinata* and *Selaginella pilifera*, Horner et al. (1975) stated that the ligule had vertical cell walls with no plasmodesmata between sheath cells and the glossopodial cells, but they did not claim that there was an endodermis or Casparian bands in the ligules. From Harvey-Gibson (1897) to Liu et al. (2022), no endodermis has been identified in *Selaginella* microphylls.

As opposed to their shoots, the situation of the roots of *Selaginella* is clearly different, as shown by us and by Damus et al.

(1997, figs. 4, 6, 12, 15–17), who show that an endodermis with distinct Casparian bands is present. This has developmental as well as evolutionary implications.

What fossils may reveal. Even literature on the fossil record of the lycopod lineage is revealing. In their evolutionary tree, Hetherington et al. (2021, fig. 6) suggest that an endodermis arose with the origin of the pathway leading directly to the extant lycopods, in spite of the fact that there has been considerable dispute about and even some evidence against an endodermis in members of the Lycopodiaceae (e.g., Damus et al. 1997). Nevertheless, Hetherington et al. (2021, figs. 3, 6) revealed axes in which there was a ring around the obvious stele in a “root-bearing axis” of *Asteroxylon mackiei* from the Rhynie Chert of the Early Devonian (397–418 mya). Furthermore, they illustrated the presumed origin of root-bearing axes and roots, including an endodermis, via dichotomies leading to the lycopods and beyond. It should be noted again that the Lycopodiaceae have adventitious roots arising laterally or vertically from stems, whereas the Selaginellaceae have roots arising from rhizophores via dichotomies (Hetherington et al. 2021; see also Imaichi and Kato 1989, 2019, etc.). Beyond the Rhynie Chert examples, other early fossils of *Lycaugea edieae* from the Late Devonian (359–385 mya) showed cell layers at the boundary of the inner cortex and the stele that could be an endodermis or endodermoid (Meyer-Berthaud et al. 2021, fig. 2A–2C, 2E–2G). Matten (1989, figs. 1–12) illustrated such a layer in the Devonian stems of *Wexfordia hookense*. The illustration of *Lycoxylon indicum* by Wikström (2001, fig. 5) showed only a ring of tissues in the inner cortex, much like our unstained or berberine images. Furthermore, Wikström (2001) stated that the split between modern *Lycopodium* and *Lycopodiella* occurred long ago, so these tissue patterns were probably established before the Lower Jurassic. Taylor et al. (2009, fig. 9.41) illustrated a Pennsylvanian (299–318 mya) lepidodendrid (*Synchysidendron*) stem and branch trace with an obvious darkened layer in their inner cortices that could easily be a ring of cells in the same position as what we have reported for extant lycopods.

Some early Middle Triassic fossil lycopods (e.g., *Hapsidoxylon terpsichorum*) show a darkened layer of cells surrounding the stele in the position of the endodermoid (McManus et al. 2002, fig. 1). Bateman et al. (2007, figs. 1–6) show somewhat similar layers of cells in the innermost cortex around a stele in the fossil lycopodialean *Hestia eremosa* that could be endodermoid. McLoughlin et al. (2015, pl. I, fig. 1, pl. III, fig. 4) labeled an endodermis in *Paurodendron stellatum*, but no Casparian band is visible in their photographs; their plate I, figure 2, however, illustrates an axis that is clearly of the selaginelloid type, with well-preserved trabeculae traversing an inner-middle cortical lacuna, but no Casparian bands. Middle Jurassic (161–175 mya) lycopod fossils of *Lycopodites hannahensis*, of the Lycopodiaceae lineage, reveal the same kind of stele as the abovenamed fossils (Thomas 2017). But in the Selaginellaceae line, the extinct *Selaginellites* (Leisman 1961) and extinct members of the genus *Selaginella* (Middle Pennsylvanian, 307–311 mya; Schlanker and Leisman 1969; Schmidt et al. 2020) reveal similar trabeculae within the cortical lacunae surrounding the singular stele or multiple steles. Kenrick and Strullu-Derrien (2014) showed that fungal colonization could have also played a major role in the development and occurrence of barrier layers in the roots of fossil groups, but without evidence of an endodermis; photos in Winther and Friedman (2008) revealed an endodermis.

An intriguing and enigmatic aspect of *Selaginella* evolution is that the ancestors are believed to have evolved in wetland environments, as one might expect for plants that evolved heterospory and needed water for reproduction while CO₂ declined (Banks 2009; Taylor et al. 2009; Bonacorsi et al. 2020, 2021). However, as Klaus et al. (2017) have shown, adaptation to xeric environments became an early trait of the *Selaginella* genus. Thus, the presence of a cuticle or cuticle-like layer around the stem stele is enigmatic since the stem epidermis has a cuticle. Little has been done since McLean and Juniper (1979) demonstrated Casparian bands in a basal trabecular cell associated with presumptive cuticle on outer trabecular cell walls in stems of *S. kraussiana*, although Gola and Jernstedt (2016) had autofluorescent images of a ring around the steles without any obvious Casparian bands. Indeed, maybe that ring of wall material around the *Selaginella* inner cortex or outer stele zone is cutinized or suberized, and maybe the ring is part of an “endodermis,” which in *Selaginella* probably arises jointly with the so-called pericycle, somewhat differently from the situation in angiosperm roots and shoots. Because we could not demonstrate them conclusively, the Casparian bands and/or the so-called trabecular ring or our endodermoid wall may not be chemically the same as those in ferns and seed plants. These features also point to the need to understand why there is air space tissue in the inner cortex of *Selaginella* stems that is bordered on the interior by a layer apparently composed of cutin or suberin (see Meyer and Peterson 2013).

Cell wall compounds, genetics, evolution. The chemical composition of the cell wall components of these important tissues has long been studied—for example, from Kroemer (1903) to Novo-Uzal et al. (2012). There has been a major effort to identify the chemical compounds that make up plant cell walls across the vascular plant spectrum (e.g., Towers and Maass 1965; Popper et al. 2001; Schreiber and Franke 2011; Novo-Uzal et al. 2012; Niklas et al. 2017; Song et al. 2019; Falcioni et al. 2022). The occurrence of unique primary cell wall compounds (Popper et al. 2001; Popper and Tuohy 2010; Espiñeira et al. 2011; Harholt et al. 2012), lignins (Towers and Maass 1965; Weng et al. 2008; Naseer et al. 2012; Novo-Uzal et al. 2012; Song et al. 2019), and cutins and suberins (Pollard et al. 2008; Yeats et al. 2012; Meyer and Peterson 2013; Song et al. 2019; Philippe et al. 2020) in the Lycopodiaceae and Selaginellaceae should be more thoroughly investigated. In particular, the lignins in lycopod walls have been shown to differ among groups of land vascular plants; for example, syringyl lignin is not present as a ring around the stem stele in *Selaginella moellendorffii* (Weng et al. 2011, fig. 6a–6c). In Novo-Uzal et al. (2012, fig. 6B), a subtle ring around the innermost trabecular cells in the lacuna of *S. martensii* does not reveal either the red of syringyl lignins or the brown of guaiacyl lignins from Maule staining, although there is a faint, uneven, greenish ring on the inner side of the lacuna/trabeculae/inner cortex. Syringyl, p-hydroxyphenyl, and guaiacyl lignins were identified in *Selaginella* by Naseer et al. (2012, fig. 4), but they found only p-hydroxyphenyl and guaiacyl lignins in “other Lycophytes.”

Conclusions

Lycopodiaceae. The two subfamilies of Lycopodiaceae differ in major structural characteristics. The Lycopodioidae have a variable endodermoid in the stems and roots that is more defined

and distinct, being mostly a layer or two of cells, with more distinct cell walls in *Diphasiastrum* and *Dendrolycopodium* than in *Lycopodiella* and *Lycopodium*. There is a root origin from the stem monostele, perpendicular across the cortex, with epidermal emergence of their adventitious roots and more sclerenchymatous cortex outside plectosteles or actinosteles, more typical of a vascular cylinder of roots; the roots become diarch in *Dendrolycopodium*. The middle cortex has much sclerenchyma.

The Huperzioidae have stems that, near the shoot tips, have endodermoid around the plectosteles and microphyll leaf traces that transitions into endodermis throughout most of the stem; microphyll leaf traces (but not microphylls); and diarch root traces, which may also have suberin lamellae in addition to Casparian bands. Adventitious roots arise from the monosteles and always traverse the cortex vertically, parallel to the steles, to have a cortical emergence; there is little thickening of the cell walls of the cortex in the stems or roots examined, except for a little in the outer cortex.

Selaginellaceae. On the other hand, Selaginellaceae can be characterized by stems with monosteles or polysteles, each surrounded by a lacuna with trabeculae or strands of cells from the edge of the stele to the middle cortex. We found no convincing evidence of an endodermis or endodermoid in the five species we examined across the Selaginellaceae, but in all species except *Selaginella lepidophylla*, there is an extracellular stele-cortex wall lining the outside of the stele and trabecular cells closest to the stele; we could not determine the chemical composition of the wall with our staining and microscopic methods, but the epidermal cuticle resembles the stele-cortex wall in laser confocal images. Rhizophores (except in *Selaginella borealis*) and dichotomized roots beyond the rhizophores have monarch vascular cylinders with distinct endodermis made up of Casparian bands and sometimes suberin lamellae. There is little sclerenchyma in the cortex.

When vascular plants started to produce the kinds of cell walls, especially lignins but also suberins and other compounds (e.g.,

Geldner 2013; Meyer and Peterson 2013, Niklas et al. 2017), that characterize lycopods (e.g., Towers and Maass 1965; Novo-Uzal et al. 2012), they did so because of the presence, coordination, and expression of their genes and so on. The enigma of the Lycopodiaceae and Selaginellaceae is that they apparently took different pathways to produce barriers to the uptake and movement of water, minerals, oxygen, carbon dioxide, pathogens, and so on as they adapted to life on land (see references on the functions and roles of the endodermis by, e.g., Brundrett and Kendrick 1990; Brundrett 2002; Geldner 2013; Meyer and Peterson 2013; Barberon 2016; Soukup and Tylová 2018; Kowal et al. 2020; Calvo-Polanco et al. 2021). From the tips of their roots to their shoot apical meristems, leaves, and reproductive structures, there are major questions about anatomy, development, and evolution that have not been resolved (Martone et al. 2009; Banks et al. 2011; Espiñeira et al. 2011; Weng et al. 2011; Harholt et al. 2012; Naseer et al. 2012; Novo-Uzal et al. 2012; Lee et al. 2013; Evkaikina et al. 2017; Niklas et al. 2017; Fang et al. 2021), and our findings point to the need for far more extensive studies of the origins of tissues, the kinds of cell wall compounds, and the presence and activity of the genes and genetic mechanisms of the stems and roots of Lycopodiaceae and Selaginellaceae, direct descendants of plants that lived hundreds of millions years ago and that others should be able to study in much greater breadth, depth, and detail.

Acknowledgments

We express our gratitude to Marilyn A. Seago, Zenab Mohamed, Doren Norfleet, Jennifer Allen, Meghan Fidler, Yulia Artemenko, Aleš Soukup, Edita Tylová, Julien Bachelier, the State University of New York at Oswego, Carl Zeiss (Thornwood, NY), and the reviewers and editors.

Literature Cited

- Arana MD, H Reinoso, AJ Oggero 2014 Morfología y anatomía de ejes caulinares, licofilos y esporangios de *Phlegmariurus phyllicifolius*: un aporte a la sistemática de las Lycopodiaceae Neotropicales. *Rev Biol Trop* 62:1217–1227.
- Banks JA 2009 *Selaginella* and 400 million years of separation. *Annu Rev Plant Biol* 60:223–238.
- Banks JA, T Nishiyama, M Hasebe, JL Bowman, M Gribskov, C Depamphilis, VA Albert, et al 2011 The *Selaginella* genome identifies genetic changes associated with the evolution of vascular plants. *Science* 332:960–963.
- Barberon M 2016 The endodermis as a checkpoint for nutrients. *New Phytol* 213:1604–1610.
- Barclay BD 1931 Origin and development of tissues in stem of *Selaginella wildenovii*. *Bot Gaz* 91:452–461.
- Bateman RM, P Kenrick, GW Rothwell 2007 Do eligulate herbaceous lycopsids occur in Carboniferous strata? *Hestia eremosa* gen. et sp. nov. from the Mississippian of Oxroad Bay, East Lothian, Scotland. *Rev Palaeobot Palynol* 144:323–335.
- Beck CB 2010 An introduction to plant structure and development. Cambridge University Press, Cambridge.
- Bhambie S 1965 Studies in pteridophytes. V. The development, structure and arrangement of leaves in some species of *Lycopodium*. *Proc Indian Acad Sci* 61:242–252.
- Bierhorst DW 1971 Morphology of vascular plants. Macmillan, New York.
- Bonacorsi NK, P Gensel, FM Hueber, AB Leslie 2021 *Ommiastrobus* gen. nov., an Emsian plant with implications for the evolution of heterospory in the Early Devonian. *Int J Plant Sci* 182:198–209.
- Bonacorsi NK, P Gensel, FM Hueber, CH Wellman, AB Leslie 2020 A novel reproductive strategy in an Early Devonian plant. *Curr Biol* 30:R371–R389.
- Bower FO 1885 On the development and morphology of *Phylloglossum drummondii*. *Philos Trans* 176:665–678.
- 1894 Studies in the morphology of spore-producing members: Equisetineae and Lycopodineae. *Philos Trans B* 185:473–572.
- Bruchmann H 1874 Ueber Anlage und Wachstum der Wurzeln von *Lycopodium* und *Isoetes*. Mauke, Jena, Germany.
- Brulé V, A Rafsanjani, M Asgari, TL Western, D Pasini 2019 Three-dimensional functional gradients direct stem curling in the resurrection plant *Selaginella lepidophylla*. *J R Soc Interface* 16:20190454.
- Brundrett MC 2002 Coevolution of roots and mycorrhizas of land plants. *New Phytol* 154:275–304.
- Brundrett MC, D Enstone, CA Peterson 1988 A berberine-aniline blue fluorescent staining procedure for suberin, lignin, and callose in plant tissue. *Protoplasma* 146:133–142.

- Brundrett M, B Kendrick 1990 The roots and mycorrhizas of herbaceous woodland plants. II. Structural aspects of morphology. *New Phytol* 114:469–479.
- Brundrett MC, DB Kendrick, CA Peterson 1991 Efficient lipid staining in plant material with Sudan red 7B or fluorol yellow 088 in polyethylene glycol-glycerol. *Biotech Histochem* 66:111–116.
- Buck WR, TW Lucansky 1976 An anatomical and morphological comparison of *Selaginella apoda* and *Selaginella ludoviciana*. *Bull Torrey Bot Club* 103:9–16.
- Calvo-Polanco M, Z Ribeyre, M Dauzat, G Reyt, C Hildago-Shrestha, P Diehl, M Frenger, et al 2021 Physiological roles of Casparian strips and suberin in the transport of water and solutes. *New Phytol* 232:2295–2307.
- Cardosa AA, D Visel, CN Kame, TA Batz, CG Sánchez, L Kaack, LJ Lamarque, et al 2020 Drought-induced lacuna formation in the stem causes hydraulic conductance to decline before xylem embolism in *Selaginella*. *New Phytol* 227:1804–1817.
- Casparry R 1858 Die Hydrillen. *Jahrb Wiss Bot* 1:377–512.
- Christenhusz MJM, X-C Zhang, H Schneider 2011 A linear sequence of extant families and genera of lycophytes and ferns. *Phyotaxa* 19:7–54.
- Chu MC-Y 1974 A comparative study of the foliar anatomy of *Lycopodium* species. *Am J Bot* 61:681–692.
- Damus M, RL Peterson, DE Enstone, CA Peterson 1997 Modification of cortical cell walls in roots of seedless vascular plants. *Bot Acta* 110:190–195.
- De Bary A 1877 Vergleichende Anatomie der Vegetationsorgane der Phanerogamen und Farne. Pages 1–663 in A De Bary, J Sachs, eds. *Handbuch der Physiologischen Botanik*. Band 3. Wilhelm Engelmann, Leipzig.
- 1884 Comparative anatomy of the vegetative organs of the phanerogams and ferns. Clarendon, Oxford.
- Dengler NG 1983 The developmental basis of anisophylly in *Selaginella martensii*. I. Initiation and morphology of growth. *Am J Bot* 70:181–192.
- Enstone DE, CA Peterson, F Ma 2003 Root endodermis and exodermis: structure, function, and responses to the environment. *J Plant Growth Regul* 28:444–455.
- Esau K 1977 Anatomy of seed plants. Wiley, New York.
- Espiñeira JM, E Novo-Uzal, LV Gómez Ros, JS Carrión, F Merino, A Ros Barceló, F Pomar 2011 Distribution of lignin monomers and the evolution of lignification among lower plants. *Plant Biol* 13:59–68.
- Evkaikina AI, L Berke, MA Romanova, EP Proux-Wéra, AN Ivanova, C Rydin, K Pawlowski, OV Voitsekhovskaja 2017 The *Huperzia selago* shoot tip transcriptome sheds new light on the evolution of leaves. *Genome Biol Evol* 9:2444–2460.
- Fahn A 1990 Plant anatomy. Pergamon, Oxford.
- Falcioni R, T Moriwaki, RH Furlanetto, MR Nanni, WC Antunes 2022 Simple, fast and efficient methods for analysing the structural, ultrastructural and cellular components of the cell wall. *Plants* 11:995.
- Fang T, H Motte, B Parizot, T Beckman 2021 Early “rootprints” of plant terrestrialization: *Selaginella* root development sheds light on root evolution in vascular plants. *Front Plant Sci* 12:735514.
- Field AR, W Testo, PD Bostock, JAM Holtum, M Waycott 2016 Molecular phylogenetics and the morphology of the Lycopodiaceae subfamily Huperzioidae supports three genera: *Huperzia*, *Phlegmariurus* and *Phylloglossum*. *Mol Phylogenet Evol* 94:635–657.
- Freeburg JA, RH Wetmore 1967 The Lycopside—a study in development. *Phytomorphology* 17:78–91.
- Friedman WE, ME Cook 2000 The origin and early evolution of tracheids in vascular plants: integration of paleobotanical and neobotanical data. *Philos Trans R Soc Lond* 355:857–868.
- Fujinami R, R Imaichi, T Yamada 2017 Root apical meristem diversity and the origin of roots: insights from extant lycophytes. *J Plant Res* 133:291–296.
- Fujinami R, A Nakajima, R Imaichi, T Yamada 2021 *Lycopodium* root meristem dynamics support homology between shoots and roots in lycophytes. *New Phytol* 229:460–468.
- Fujinami R, T Yamada, R Imaichi 2020 Root apical meristem diversity and the origin of roots: insights from extant plants. *J Plant Res* 133:291–296.
- Geldner N 2013 The endodermis. *Annu Rev Plant Biol* 64:531–558.
- Gifford EM, AS Foster 1989 Morphology and evolution of vascular plants. W. H. Freeman, New York.
- Gola EM, JA Jernstedt 2011 Impermanency of initial cells in *Huperzia lucidula* (Huperziaceae) shoot apices. *Int J Plant Sci* 172:847–853.
- 2016 Vascular structure contributes to shoot sectoriality in *Selaginella kraussiana*. *Acta Soc Bot Pol* 85:3515.
- Gola EM, JA Jernstedt, B Zagórska-Marek 2007 Vascular architecture in shoots of early divergent vascular plants, *Lycopodium clavatum* and *Lycopodium annotinum*. *New Phytol* 174:774–786.
- Grego-Valencia D, T Terrazas, JD Tejero-Díez, R Lara-Martínez, LF Jiménez-García, S Aguilar-Rodríguez 2018 Variación anatómica del tallo y ultraestructura de la membrana de la punteadura en los elementos traqueales de *Selaginella pallescens* (Selaginellaceae). *Bot Sci* 96:662–667.
- Harholt J, I Sørensen, J Fangel, A Roberts, WGT Willats, H Vibe Scheller, B Larsen Petersen, JA Banks, P Ulvskov 2012 The glycosyltransferase repertoire of the spikemoss *Selaginella moellendorffii* and a comparative study of its cell wall. *PLoS ONE* 7:e35846.
- Harrison CJ, JL Morris 2017 The origin and early evolution of vascular plant shoots and leaves. *Philos Trans R Soc B* 373:20160496.
- Harrison CJ, M Rezvani, JA Langdale 2007 Growth from two transient apical initials in the meristem of *Selaginella kraussiana*. *Development* 134:881–889.
- Harvey-Gibson RJ 1894 Contributions towards a knowledge of the anatomy of the genus *Selaginella*, Spr. I. The stem. *Ann Bot* 8:133–206.
- 1896 Contributions towards a knowledge of the anatomy of the genus *Selaginella*, Spr. I. The ligula. *Ann Bot* 10:77–88.
- 1897 Contributions towards a knowledge of the anatomy of the genus *Selaginella*, Spr. III. The leaf. *Ann Bot* 11:123–155.
- 1902 Contributions towards a knowledge of the anatomy of the genus *Selaginella*. IV. The root. *Ann Bot* 16:449–466.
- Hegelmair F 1872 Zur Morphologie der Gattung *Lycopodium*. *Bot Ztg* 30:773–779, 789–801, 805–819, 825–834, 837–850.
- Heimsch C, JL Seago Jr 2008 Organization of the root apical meristem in angiosperms. *Am J Bot* 95:1–21.
- Hetherington AJ, SL Bridson, AL Jones, H Hass, H Kerp, L Dolan 2021 An evidence-based 3D reconstruction of *Asteroxylon mackiei*, the most complex plant preserved from the Rhynie Chert. *eLife* 10:e69447.
- Hill JB 1914 The anatomy of six epiphytic species of *Lycopodium*. *Bot Gaz* 58:61–85.
- 1919 Anatomy of *Lycopodium reflexum*. *Bot Gaz* 68:226–231.
- Horner HT, CK Beltz, R Jagels, RE Boudreau 1975 Ligule development and fine structure in two heterophyllous species of *Selaginella*. *Can J Bot* 53:127–143.
- Hoysted GA, MI Bidartondo, JG Duckett, S Pressel, KJ Field 2020 Phenology and function in lycopod-Mucoromycotina symbiosis. *New Phytol* 229:2389–2394.
- Imaichi R, R Hiratsuka 2007 Evolution of shoot apical meristem structures in vascular plants with respect to plasmodesmatal network. *Am J Bot* 94:1911–1921.
- Imaichi R, M Kato 1989 Developmental anatomy of the shoot apical cell, rhizophore and root of *Selaginella uncinata*. *Bot Mag Tokyo* 102:369–380.
- Imaichi R, N Moritoki, HK Solvang 2019 Evolution of root apical meristem structures in vascular plants: plasmodesmatal networks. *Am J Bot* 105:1453–1468.
- Jacobs WP 1988 Development of procambium, xylem, and phloem in the shoot apex of *Selaginella*. *Bot Gaz* 149:64–70.
- Jeffrey EC 1902 The structure and development of the stem in the peridophyta and gymnosperms. *Philos Trans R Soc Lond* 195:119–146.
- Jones CE 1905 II. The morphology and anatomy of the stem of the genus *Lycopodium*. *Trans Linn Soc Bot* 7:15–35.

- Kaplan DR 2022 Kaplan's principles of plant morphology. CD Specht, ed. CRC, Boca Raton, FL.
- Karrfalt EE 1981 The comparative and developmental morphology of the root system of *Selaginella selaginoides* (L.) Link. *Am J Bot* 68:244–253.
- Kenrick P 2002 The origin of roots. Pages 1–13 in Y Waisel, A Eshel, U Kafkali, eds. *Plant roots: the hidden half*. Marcel Dekker, New York.
- Kenrick P, PR Crane 1997 The origins and early evolution of plants on land. *Nature* 389:33–39.
- Kenrick P, C Strullu-Derrien 2014 The origin and early evolution of roots. *Plant Physiol* 166:570–580.
- Kessler E 2009 Esporófito de *Huperzia mandiocana* (Raddi) Trevisan (Lycopodiaceae): morfoanatomia e ontogenese. PhD diss, Universidade Federal de Santa Catarina, Florianópolis, Brazil.
- Klaus KV, C Schulz, DS Bauer, T Stützel 2017 Historical biogeography of the ancient lycophyte genus *Selaginella*: early adaptation to xeric habitats on Pangea. *Cladistics* 33:469–480.
- Kowal J, E Arrigoni, J Serra, M Bidartondo 2020 Prevalence and phenology of fine root endophyte colonization across populations of *Lycopodiella inundata*. *Mycorrhiza* 30:577–587.
- Kroemer K 1903 Wurzelhaut: Hypodermis und Endodermis der Angiospermenwurzel. *Bibl Bot* 12:1–159.
- Lee Y, MC Rubio, J Allassimone, N Geldner 2013 A mechanism for localized lignin deposition in the endodermis. *Cell* 153:402–412.
- Lehnert M, M Kriug, M Kessler 2016 A review of symbiotic fungal endophytes in lycopohytes and ferns: a global phylogenetic and ecological perspective. *Symbiosis* 71:77–89.
- Leisman G 1961 Further observations on the structure of *Selaginellites crassincinctus*. *Am J Bot* 48:224–229.
- Liu J-W, C-L Huang, IA Valdespino, J-F Ho, T-Y Lee, P Chesson, C-R Sheue 2022 Morphological and phylogenetic evidence that the novel leaf structures of multivein *Selaginella schaffneri* are derived traits. *Flora* 286:151976.
- Lu P, JA Jernstedt 1996 Rhizophore and root development in *Selaginella martensii* meristem transitions and identity. *Int J Plant Sci* 157:180–194.
- Lux A, M Baláz, M Kummerová, A Soukup, O Votrubová, J Abe, S Morita, T Rost 2017 Visual guide to plant anatomy. Academia, Prague.
- Lux A, S Morita, J Abe, K Ito 2005 An improved method for clearing and staining free-hand sections and whole-mount samples. *Ann Bot* 96:989–996.
- Martone PT, JM Estevez, F Lu, K Ruel, MW Denny, C Somerville, J Ralph 2009 Discovery of lignin in seaweed reveals convergent evolution of cell-wall architecture. *Curr Biol* 19:169–175.
- Matten LC 1989 A petrified lycopod from the uppermost Devonian of Hook Head, County Wexford, Ireland. *Bot Gaz* 150:323–336.
- McLean B, BE Juniper 1979 The fine structure and development of the trabeculae and the trabecular ring in *Selaginella kraussiana*. *Planta* 145:443–448.
- McLoughlin S, AN Drinnan, BJ Slater, J Hilton 2015 *Paurodendron stellatum*: a new Permian permineralized herbaceous lycopsid from the Prince Charles Mountains, Antarctica. *Rev Palaeobot Palynol* 220:1–15.
- McManus HA, L Boucher, EL Taylor, TN Taylor 2002 *Hapsidoxylon terpsichorum* gen. et sp. nov., a stem with unusual anatomy from the Triassic of Antarctica. *Am J Bot* 89:1958–1966.
- Meyer CJ, CA Peterson 2013 Structure and function of three suberized cell layers: epidermis, exodermis, and endodermis. Pages 5.1–5.20 in A Eshel, T Beeckman, eds. *Plant roots, the hidden half*. CRC, Boca Raton, FL.
- Meyer-Berthaud B, A-L Decombeix, R Blanchard 2021 *Lycaugea edieae* gen. et sp. nov., a Late Devonian lycopsid from New South Wales, Australia. *Int J Plant Sci* 182:418–429.
- Mitchell G 1910 Contributions to the anatomy of *Selaginella*. V. *Ann Bot* 24:19–33.
- Mower JP, P-F Ma, F Grewe, A Taylor, TP Michael, R Van Buren, Y-L Qiu 2019 Lycophyte plastid genomics: extreme variation in GC, gene and intron content and multiple inversions between a direct and inverted orientation of the rRNA repeat. *New Phytol* 222:1061–1075.
- Naseer S, Y Lee, C Lapierre, R Franke, C Nawrath, N Geldner 2012 Casparian strip diffusion barrier in *Arabidopsis* is made of a lignin polymer without suberin. *Proc Natl Acad Sci USA* 109:10101–10106.
- Niklas KJ, ED Cobb, AJ Matas 2017 The evolution of hydrophobic cell wall biopolymers: from algae to angiosperms. *J Exp Bot* 68:5261–5269.
- Novo-Uzal E, F Pomar, LV Gómez Ros, JM Espiñeira, A Ros Barceló 2012 Evolutionary history of lignins. *Adv Bot Res* 61:309–350.
- Ogura Y 1972 Comparative anatomy of vegetative organs of the pteridophytes. Borntraeger, Berlin.
- Otręba P, EM Gola 2011 Specific intercalary growth of rhizophores and roots in *Selaginella kraussiana* (Selaginellaceae) is related to unique dichotomous branching. *Flora* 206:227–232.
- Pauluzzi G, F Divol, J Puig, E Guiderdoni, A Dievart, C Périn 2012 Surfing along the root ground tissue gene network. *Dev Biol* 365:14–22.
- Philippe G, B Sorensen, C Jiao, X Sun, Z Fei, DS Domozych, JKC Rose 2020 Cutin and suberin: assembly and origins of specialized lipidic cell wall scaffolds. *Curr Opin Plant Biol* 55:11–20.
- Pita PB, NL de Menezes, J Prado 2006 Morfologia externa e interna de raiz e caule de espécies de *Huperzia* Bernh. (Lycopodiaceae—Pteridophyta) do Brasil. *Hoehnea* 33:495–510.
- Pollard M, F Beisson, Y Li, JB Ohlrogge 2008 Building lipid barriers: biosynthesis of cutin and suberin. *Trends Plant Sci* 13:236–246.
- Popper ZA, IH Sadler, SC Fry 2001 3-O-methyl-D-galactose residues in lycophyte primary cell walls. *Phytochemistry* 57:711–719.
- Popper ZA, MG Tuohy 2010 Beyond the green: understanding the evolutionary puzzle of plant and algal cell walls. *Plant Physiol* 153:373–383.
- PPG (Pteridophyte Phylogeny Group) 2016 A community-derived classification for extant lycophytes and ferns. *J Syst Evol* 54:563–603.
- Rafsanjani A, V Brulé, TL Weatern, D Pasini 2015 Hydro-responsive curling of the resurrection plant *Selaginella lepidophylla*. *Sci Rep* 5:8064.
- Raven JA, D Edwards 2001 Roots: evolutionary origins and biogeochemical significance. *J Exp Bot* 52:381–401.
- Roberts EA, SD Herty 1934 *Lycopodium complanatum* var. *Flabelliforme* Fernald: its anatomy and a method of vegetative propagation. *Am J Bot* 21:688–697.
- Roy H, S Baruah, R Saikia, SK Borthakur 2013 *Phlegmariurus vernicosus* (Hooker & Greves) A. Löve & D. Löve (Lycopodiaceae): a new record for Northeast India. *Pleione* 7:583–588.
- Sachs J 1882 Text-book of botany, morphological and physiological. Clarendon, Oxford.
- Schlanker CM, GA Leisman 1969 The herbaceous Carboniferous lycopod *Selaginella fraiponti* comb. nov. *Bot Gaz* 130:35–41.
- Schmidt AR, L Regalado, S Weststrand, P Korall, E-M Sadowski, H Schneider, E Jansen, et al 2020 *Selaginella* was hyperdiverse already in the Cretaceous. *New Phytol* 228:1176–1182.
- Schneider EL, S Carlquist 2000a SEM studies on the vessels of heterophyllous species of *Selaginella*. *Bull Torrey Bot Soc* 127:263–270.
- 2000b SEM studies on vessels of the homosporous species of *Selaginella*. *Int J Plant Sci* 161:967–974.
- Schreiber L 1996 Chemical composition of Casparian strips isolated from *Clivia miniata* Reg. roots: evidence for lignin. *Planta* 199:596–601.
- Schreiber L, RB Franke 2011 Endodermis and exodermis in roots. eLS. <https://doi.org/10.1002/9780470015902.a0002086.pub2>.
- Schreiber L, K Hartmann, M Skrabs, J Zeier 1999 Apoplastic barriers in roots: chemical composition of endodermal and hypodermal cell walls. *J Exp Bot* 50:1267–1280.
- Schulz A, DP Little, DW Stevenson, D Bauer, C Moloney, T Stützel 2010 An overview of the morphology, anatomy, and life cycle of a new model species: the lycophyte *Selaginella apoda* (L.) Spring. *Int J Plant Sci* 171:693–712.

- Scott DH 1904 An introduction to structural botany. II. Flowerless plants. A & C Black, London.
- Seago JL Jr 2020 Revisiting the occurrence and evidence of endodermis in angiosperm shoots. *Flora* 273:151709.
- Seago JL Jr, DD Fernando 2013 Anatomical aspects of angiosperm root evolution. *Ann Bot* 112:223–238.
- Seago JL Jr, LC Marsh 1989 Adventitious root development in *Typha glauca*, with emphasis on the cortex. *Am J Bot* 76:909–923.
- Seago JL Jr, CA Peterson, DE Enstone, CA Scholey 1999 Development of the endodermis and hypodermis of *Typha glauca* Godr. and *Typha angustifolia* L. roots. *Can J Bot* 77:122–134.
- Sinnott EW 1909 On mesarch structure in *Lycopodium*. *Bot Gaz* 48:138–145.
- Song C, W Shen, L Du, J Wen, J Lin, R Li 2019 Development and chemical characterization of Casparian strips in the roots of Chinese fir (*Cunninghamia lanceolata*). *Trees* 33:827–836.
- Soukup A 2014 Selected simple methods of plant cell wall histochemistry and staining for light microscopy. Pages 27–42 in F Cvrčková, V Žárský, eds. Plant cell morphogenesis. *Methods in Molecular Biology*. Humana, New York.
- Soukup A, E Tylová 2018 Apoplastic barriers: their structure and function from a historical perspective. Pages 155–183 in VP Sahi, F Baluška, eds. *Concepts in cell biology: history and evolution*. Plant Cell Monographs. Vol 23. Springer, Cham.
- Spencer V, ZN Venza, CJ Harrison 2021 What can lycophytes teach us about plant evolution and development? modern perspectives on an ancient lineage. *Evol Dev* 23:174–196.
- Steeves TA, IM Sussex 1989 Patterns in plant development. Cambridge University Press, Cambridge.
- Stevens PF 2021 Angiosperm phylogeny website. <http://www.mobot.org/MOBOT/research/APweb/>.
- Stevenson DW 1976 Observations on phyllotaxis, stelar morphology, the shoot apex and gemmae of *Lycopodium lucidulum* Michaux (Lycopodiaceae). *Bot J Linn Soc* 72:81–100.
- Stokey AG 1907 The roots of *Lycopodium pithyoides*. *Bot Gaz* 44:57–63.
- Strasburger E, F Noll, H Schenck, G Karsten 1908 A textbook of botany. Macmillan, London.
- Suganya S, V Irudayaraj, M Johnson 2011 Pharmacognostical studies on an endemic spike-moss *Selaginella tenera* (Hook. & Grev.) Spring from the Western Ghats, South India. *J Chem Pharm Res* 3:721–731.
- Taylor TN, EL Taylor, M Krings 2009 Paleobotany, the biology and evolution of fossil plants. Elsevier, Burlington, MA.
- Thomas BA 1992 Paleozoic herbaceous lycopsids and the beginnings of extant *Lycopodium* sens. lat. and *Selaginella* sens. lat. *Ann Mo Bot Gard* 79:623–631.
- 2017 The occurrence of *Lycopodites hannahensis* Harris in the Yorkshire Jurassic together with details of its anatomy. *Proc Yorks Geol Soc* 61:281–283.
- Towers GHN, WSG Maass 1965 Phenolic acids and lignins in the Lycopodiales. *Phytochemistry* 4:57–66.
- Turner JJ 1924 Origin and development of vascular system of *Lycopodium lucidulum*. *Bot Gaz* 78:215–225.
- Uphof JCT 1920 Physiological anatomy of xerophytic *Selaginellas*. *New Phytol* 19:101–131.
- Van Tieghem P, H Douliot 1886 Sur les tiges a plusieurs cylindres centraux. *Bull Soc Bot Fr* 33:213–216.
- Vasco A, TI Smalls, SW Graham, ED Cooper, GK-S Wong, DW Stevenson, RCMoran, BA Ambrose 2016 Challenging the paradigms of leaf evolution: Class III HD-Zips in ferns and lycophytes. *New Phytol* 212:745–758.
- von Guttenberg H 1943 Die physiologischen Scheiden. *Handbuch der Pflanzenanatomie*. Abteil 1, Teil 2, Band V. Borntraeger, Berlin.
- Webster TR, R Jagels 1977 Morphology and development of aerial roots of *Selaginella martensii* grown in moist containers. *Can J Bot* 55:2149–2158.
- Webster TR, TA Steeves 1963 Morphology and development of the root of *Selaginella densa*. *Phytomorphology* 13:367–376.
- 1964 Developmental morphology of the root of *Selaginella kraussiana* A. Br. and *Selaginella wallacei* Hieron. *Can J Bot* 42:1665–1676.
- 1967 Developmental morphology of the root of *Selaginella martensii*. *Can J Bot* 45:395–404.
- Weng J-K, T Akiyama, J Ralph, C Chapple 2011 Independent recruitment of an O-methyltransferase for syringyl lignin biosynthesis in *Selaginella moellendorffii*. *Plant Cell* 23:2708–2724.
- Weng J-K, J Stout, C Chapple 2008 Independent origins of syringyl lignin in vascular plants. *Proc Natl Acad Sci USA* 105:7887–7892.
- Wernham HF 1910 The morphology of *Phylloglossum drummondii*. *Ann Bot* 24:335–347.
- Weststrand S, P Korall 2016 Phylogeny of Selaginellaceae: there is value in morphology after all! *Am J Bot* 103:2136–2159.
- Wigglesworth G 1907 The young sporophytes of *Lycopodium complanatum* and *Lycopodium clavatum*. *Ann Bot* 21:211–236.
- Wikström N 2001 Diversification and relationships of extant homosporous lycophytes. *Am Fern J* 91:150–165.
- Wilder GJ 1970 Structure of tracheids in three species of *Lycopodium*. *Am J Bot* 57:1093–1107.
- Winther JL, WE Freidman 2008 Arbuscular mycorrhizal associations in Lycopodiaceae. *New Phytol* 177:790–801.
- Yeats TH, LBB Martin, HM-F Viart, T Isaacson, Y He, L Zhao, AJ Matas, et al 2012 The identification of cutin synthase: formation of the plant polyester cutin. *Nat Chem Biol* 8:609–611.
- Zelko I, A Lux, T Sterckeman, M Martinka, K Kollárová, D Lišková 2012 An easy method for cutting and fluorescent staining of thin roots. *Ann Bot* 110:475–478.
- Zhang M-H, Q-P Xiang, X-C Zhang 2022 Plastid phylogenomic analyses of the *Selaginella sanguinolenta* group (Selaginellaceae) reveal conflict signatures resulting from sequence types, outlier genes, and pervasive RNA editing. *Mol Phylogenet Evol* 173:107507.
- Zhou X-M, CJ Rothfels, L Zhang, Z-R He, TL Péchon, H He, NT Lu, et al 2016 A large-scale phylogeny of the lycophyte genus *Selaginella* (Selaginellaceae: Lycopodiopsida) based on plastid and nuclear loci. *Cladistics* 32:360–389.
- Zhou X-M, L-B Zhang 2015 A classification of *Selaginella* (Selaginellaceae) based on molecular (chloroplast and nuclear), macromorphological, and spore features. *Taxon* 64:1117–1140.